The analogous condition under which $b_n \sim b_n^s$ leads to a less severe criterion on N'; that is a smaller N' for a given thickness and wavelength. Finally we use the fact that the greatest value of n for which these expressions were derived is subject to the inequality $(n+1)^2 \ll |N_2\nu|$. Hence $(n+1)/\nu$ can be replaced by $\frac{1}{2}|N_2| = N'/\sqrt{2}$ on the right side to obtain a criterion independent of n. This leads to

$$N' > \frac{1}{2\sqrt{2}} \frac{\mu_2}{\mu_3} \frac{1}{(\nu - \alpha)}$$

or in terms of conductivity s_2

$$s_2 > \left(\frac{\mu_2}{\mu_3}\right)^2 \frac{1}{4\mu_2\omega} \frac{1}{(b-a)^2}.$$

By solving for $b-a$ this criterion can also be interpreted to say that if $b-a$ exceeds

$$\frac{1}{2\sqrt{2}} \frac{\mu_2}{\mu_3}$$

times the skin depth the Rayleigh return will be like that of a solid perfectly conducting sphere.

For an illustrative numerical example we assume $\mu_1 = \mu_2 = \mu_3 = 4\pi \times 10^{-7}$ henry/meter, the value for free space. Then for s_2 in mhos/m, $(b-a)$ in meters and f in cycles/second

$$s_2 > \frac{10^7}{4\pi(b-a)^2\omega} \sim \frac{1.3 \times 10^5}{(b-a)^2 f}.$$

Let us consider a 0.5-mm thick shell. Then

$$s_2 > \frac{10^{11}}{f}$$

is required. For 3-cm waves, $f = 10^{10}$ and the requirement is $s_2 > 10$ mhos/m, while for 3-meter waves, $f = 10^8$ and the requirement is $s_2 > 1000$ mhos/m. s_2 is very frequency sensitive for dielectrics and $s_2 = 10$ is just about the greatest value of s_2 reached for 3-cm waves by unloaded dielectrics listed in von Hippel's tables. It is greater than the values reached for $f = 10^8$ so that for 3-meter waves and a 0.5-mm thickness some loading of the dielectrics would be needed.

ACKNOWLEDGMENT

We should like to acknowledge the support given this program by Air Force Cambridge Research Center, Bedford, Mass., and Rome Air Development Center, Griffiss AFB, N. Y., under contracts AF19(602)-4993, AF30(602)-1853 and AF30(602)-1808.

We also wish to acknowledge the assistance of members of the Radiation Laboratory of The University of Michigan, Ann Arbor; T. B. A. Senior for aid on theoretical parts of this investigation, and A. Olte, D. L. Pepper, T. E. Hon, E. F. Knott and R. L. Wolford for assistance in the experimental work. We wish to thank our reviewers for many useful and stimulating criticisms of the original manuscript.

Correspondence

Epitaxial Diffused Transistors*

This letter describes diffused base transistors, the structures of which incorporate thin semiconductor layers epitaxially deposited on low-resistivity substrates of the same semiconductor. Collector series resistance and excess stored charge in the saturated switching condition are substantially lower than for diffused base transistors made by more conventional techniques. This makes possible significant increases in switching speed and high-frequency gain. The technique promises comparable improvements in diode speeds and opens possibilities of new complex structures.

The bulk resistivity of the semiconductor wafer used in conventional diffused base mesa transistors gives rise to an internal resistance in series with the collector. In small signal transmission applications of the transistor, this resistance reduces the high-frequency gain by absorbing power which might otherwise be coupled to the load. In switching or other large signal use, it causes excessive "on" voltage drop. In addition, the high-resistivity bulk region slows the recovery of the transistor from a saturated switching condition by providing a long-lifetime medium for stored charge. It is ordinarily not possible to suppress these effects by use of low-resistivity wafers because this also lowers the collector breakdown voltage and raises the collector capacitance.

A more ideal transistor structure is shown in Fig. 1. Here, the junction characteristics are controlled by diffusing the base and emitter layers into a thin, high-resistivity layer. The main body of the collector is a very-low-resistivity material. Such a structure possesses all the advantages of conventional diffused base mesa transistors and eliminates many of the disadvantages.

A technique for making such structures is now available. The thin high-resistivity layer can be produced by thermal decomposition of silicon tetrachloride or germanium tetrachloride on a low-resistivity

* Received by the IRE, July 5, 1960.

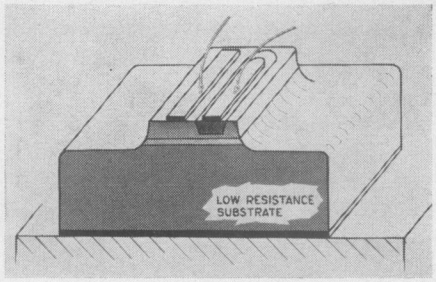

Fig. 1—Mesa transistor structure with thin high-resistivity layer between diffused collector junction and low-resistance collector body.

TABLE I

MEDIUM-POWER SILICON MESA TRANSISTORS
T_s (STORAGE TIME CONSTANT) FROM
STORAGE TIME RELATION

$$t_s = T_s \ln\left(\frac{\beta I_{B1}}{I_c}\right) \text{ WITH } I_{B2} = 0$$

	Conventional Structure	Epitaxial Film Structure
Substrate Resistivity	—	0.002 Ω cm
Epitaxial Film Resistivity	—	1.5 Ω cm
Emitter Size	4×35	2×20 mil²
BV_{CBO}	80	90 volts
$C_C(V_{CB}=5V)$	30	10 μμf
$V_{CE}(I_C=500$ ma $I_B=50$ ma)	1.9	0.6 volts
T_S	1350	100 mμsec

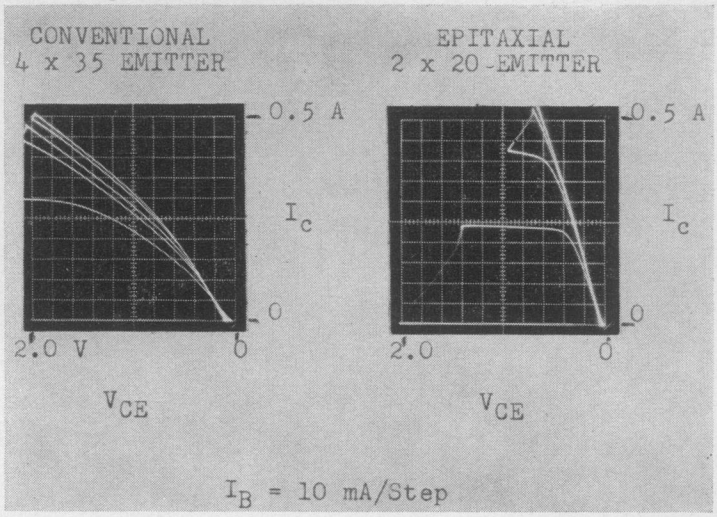

Fig. 2—Low-voltage common emitter output characteristics of conventional and epitaxial silicon (medium-power, *n-p-n*) mesa transistors.

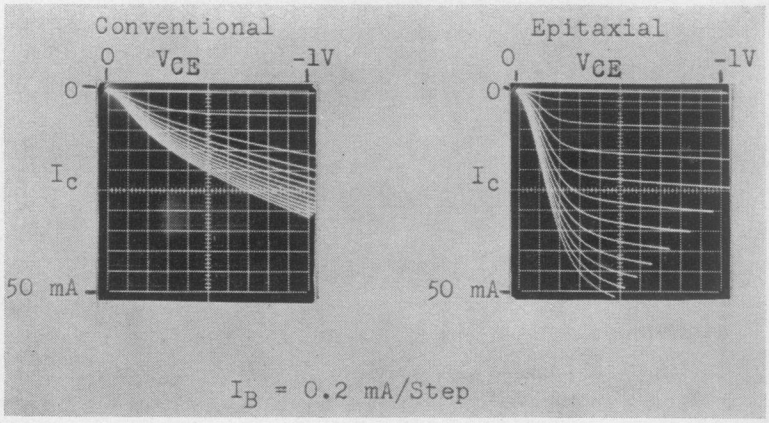

Fig. 3—Low-voltage common emitter output characteristics of conventional and epitaxial germanium mesa transistors. (Emitter 1×2 mil².)

substrate of the same material. When carried out under the proper conditions, the layers grow epitaxially; *i.e.*, the single crystal structure of the substrate is propagated into the thin film. Conventional diffused base technology can then be used to make transistors on this material.

Rough approximations to the structure of Fig. 1 have previously been obtained by diffusing or alloying a low-resistivity region into the wafer from the collector contact side. Because the critical thickness of the high-resistivity region is the difference between total wafer thickness and the depth of alloying or diffusion, these procedures have been difficult to control and therefore expensive.

Transistors of both germanium and silicon have been made on epitaxial material. In the case of silicon, a low-resistivity (0.002 ohm-cm) *n*-type crystal was used as a substrate. Epitaxial *n*-type layers several microns thick were produced by the decomposition of $SiCl_4$. The base and emitter layers were then diffused using conventional boron and phosphorus processes. The transistors have all the desirable features of conventional diffused base transistors. For example, they have high alpha, high gain and sharp junctions. None of the electrical parameters were degraded, while some parameters have been improved. Comparison data for two medium power silicon transistors with about equal power ratings are given in Table I, and their collector characteristics are shown in Fig. 2. One is a conventional 0.5-ampere switching transistor. The other is an epitaxial diffused transistor with a much smaller emitter area. As anticipated, the collector series resistance, switching speed and collector capacitance of the epitaxial transistor are significantly better than for the conventional transistor. Comparable and extended results have been obtained for low-level silicon switching transistors by A. E. Blakeslee and H. J. Patterson.

Similar improvements have been made in germanium transistors. In this case the epitaxial layer was again formed on a low-resistivity substrate by decomposition of the tetrachloride. The base and emitter layers were formed by diffusing antimony and alloying aluminum, respectively. The collector characteristics of a typical unit as compared with a conventional structure are shown in Fig. 3.

In addition to the improvements in electrical performance, many fabrication problems are eased by use of epitaxially grown material. For example, the problem of making noninjecting ohmic contacts to the collector body of a germanium transistor is eliminated. Also, in fabricating the epitaxial transistor structures, there is no need to lap or polish the wafer prior to diffusion. By the elimination of these processes, mechanical damage in the material is reduced. In addition, the epitaxial layer provides close control of the high-resistivity region of the collector body.

Although we have emphasized the compatibility of epitaxial films with conventional diffusion and alloying processes, the use of the material is by no means restricted to these techniques. For example, the need for a diffused base layer may be eliminated by doping the epitaxially grown film to an appropriate resistivity.

The same techniques obviously apply to diodes, *p-n-p-n* devices and similar junction elements. Comparable improvements are expected in these devices.

The use of epitaxial material, however, is not restricted to conventional devices. Complex structures, which are difficult to fabricate or not possible with conventional device technology now become feasible. These techniques will open many new horizons in the semiconductor device area.

The authors gratefully acknowledge the help of their colleagues in this work. The guidance and assistance of I. M. Ross, J. M. Early, and J. M. Goldey is especially appreciated.

H. C. THEUERER
J. J. KLEIMACK
H. H. LOAR
H. CHRISTENSEN
Bell Telephone Labs.
Murray Hill, N. J.

Use of the Hydrogen Line to Measure Vehicular Velocity*

The purpose of this correspondence is to present some of the considerations leading to the development of a device to measure the velocity of a vehicle by means of the Doppler shift in the stellar spectrum.

In 1947, the first laboratory measurements of the 21-cm hydrogen line in radio astronomy were made.[1] In 1955, the "red shift" of a distant radio source was detected by observing the 1420-mc absorption line Doppler shifted to 1340 mc.[2] To the present, sufficient data have been gathered on celestial radio sources so as to make it practical to employ the Doppler shift of their absorption spectra in the solution of navigation problems. Equipment is now being constructed to further study these sources for this special application. The celestial sources most highly regarded for their utility in navigation are Cassiopeia A, Taurus A and Sagittarius A. The closest of these (Taurus A) is 1100 parsecs from our planetary system, which is equivalent to approximately 3600 light years. These sources have several important physical characteristics in common. As discrete radio sources they each subtend an angle in the sky of approximately 6 minutes of arc. Their spectra may be observed both in emission and absorption. The absorption notch is quite sharp and is the basis for their utility in navigation. (It is a hydrogen cloud positioned between the observer and the radio source which causes the absorption feature to be formed.) For example, Cassiopeia A has a notch which is 25 kc wide at the half-power level. In emission, it is a line approximately 0.5 mc in width. This broadening is due to the turbulence of the hydrogen cloud whose subtended angle may be 10° of arc or more. The gross motion of the clouds represent radial velocities varying from −1 km/sec to 10 km/sec. This will Doppler shift the absorption notch 4735 cps per km/sec. The gross radial velocity of the absorbing medium may be regarded as constant over the period of an interplanetary voyage. The right ascensions of Cassiopeia A, Taurus A and Sagittarius A are 23 hours 21 minutes, 5 hours 31 minutes and 17 hours 43 minutes, respectively. Cassiopeia A and Taurus A may be found at declinations of 58° 32′ and 22° 00′ above the celestial equator, while Sagittarius is 28° 45′ below it.[3] This spacial distribution is favorable with regard to a determination of inertial velocity from three independent noncoplanar velocity measurements.

Of the three sources considered, Cassiopeia A has the greatest apparent intensity, and it is the only source which is continuously visible by an observer on earth at a latitude of +40°. Cassiopeia further lends itself to the navigation problem by having a fine absorption line approximately 200°K deep as measured with an antenna aperture of 75 feet. One may estimate the error in determining the center frequency of this fine absorption line with the use of the expression

$$\sigma_f = 2.94 \left(\frac{W}{T}\right)^{1/2} \times \frac{N}{S},$$

where

σ_f = the rms error in determining the center frequency of the notch;
W = spectrum bandwidth at the half-power level (25 kc);
T = the smoothing time (500 seconds);
N/S = noise-to-signal ratio (7);

$$\sigma_f = 2.94 \left(\frac{25 \times 10^3}{500}\right)^{1/2} \times 7$$

$$= 150 \text{ cps}.$$

This corresponds to a velocity of 70 mph.

The above equation is derived from relations given by Schultheiss *et al.*[4] for measuring the center frequency of a symmetrical power spectrum. The bandwidth is half power bandwidth for the narrow absorption line in the profile of Cassiopeia A. The time of integration, T, is taken as a period which is small compared to the duration of an interplanetary voyage. The N/S ratio is a function of the intensity of the source, size of the antenna and the noise figure of the receiver. This uncertainty is attainable with a receiver whose noise figure is of the order of 7.5 db. With the use of a maser preamplifier, the noise figure will be considerably improved with a corresponding increase in the accuracy of measurement. For a comparison between celestial sources, it is indicated by a theoretical analysis that with a 30-foot antenna, a maser preamplifier, and a smoothing time of 21 seconds, σ_v would be 200 miles per hour, using Cassiopeia A as a source. The same system, using Taurus A as a source and a smoothing time of 26 seconds, gives a σ_v of 2000 miles per hour.

In order to obtain information pertinent to the design of an automatic hydrogen line tracker which will continuously measure the radial velocity of a vehicle with respect to a celestial source, a receiver-recording system is under construction. This will produce information on the statistical nature of the hydrogen line signal. The signal is "recorded live" on a wide-band magnetic tape recorder. A portion of the black body radiation continuum of the celestial source is also recorded. These two samples are 200 kc wide and approximately 1 mc apart. Since the continuum radiation has a constant power spectral density it is used as a reference signal in an AGC circuit to compensate for the non-flatness of the receiver-recorder system. The need for this becomes obvious when one realizes that with a receiver with a 7.5-db noise figure, the absorption notch in Cassiopeia A represents a narrow depression at most only 0.5 db below the power spectral density of the background noise. In addition to a live tape recording of the hydrogen spectrum, a pen-type recording of the profile of the notch is also made. It is expected that the basic information about these stellar spectra needed to design the frequency tracker will be derived from these recordings. The live recording will then be used as a "star simulator" during tracker tests.

Basically, the hydrogen line frequency tracker will be a 1420-mc receiver. The resonance feature of the received signal will be amplified by a low-noise RF amplifier such as a maser. This is mixed with a local oscillator signal f_{LO}. The intermediate frequency $f_v - f_{LO}$ is interpreted as a zero speed with respect to the local standard of rest. The velocity of the vehicle along the line of sight to the celestial source is given by[5]

$$V = \frac{f_v - f_{LO}}{1420.40576 \text{ mc}} C$$

where

C = velocity of light
f_v = measured center frequency of notch.

Two other velocity determinations are made with respect to the two other sources. The three velocity components are fed into a computer whose output is the inertial velocity of the vehicle. These data are compared with a stored velocity program for the voyaging vehicle, and the difference used to correct velocity components of the vehicle while in flight.

SEYMOUR FELDON
GPL Division
General Precision, Inc.
Pleasantville, N. Y.

* Received by the IRE, February 29, 1960.

[1] H. C. Van De Hulst, "Studies of the 21-cm Line and their Interpretation," International Astronomical Union Symp., Cambridge University Press, England, p. 3; 1957.

[2] F. T. Haddock, "Introduction to radio astronomy," PROC. IRE, vol. 46, pp. 3–12; January, 1958.

[3] J. P. Hagen, A. E. Lilley, and E. F. McClain, "Absorption of 21-cm radiation by interstellar hydrogen," *Astrophys. J.*, vol. 122, pp. 361–375; November, 1955.

[4] P. M. Schultheiss, C. A. Wogrin, and F. Zweig, "Short time frequency measurement of narrow-band random signals in the presence of wide-band noise," *J. Appl. Phys.*, vol. 25, pp. 1025–1036; August, 1954.

[5] Frequency 1420.40576 mc, cited by A. H. Barrett, "Spectral lines in radio astronomy," PROC. IRE, vol. 46, pp. 250–259; January, 1958. See second paragraph, p. 256.

Internal Field Emission and Low Temperature Thermionic Emission into Vacuum*

Mead has recently reported on tunnel-emission experiments using aluminum oxide sandwiched between two aluminum layers.[1] This note is to report independent work along similar lines by the writer.

The objective of the work is a cold cathode possessing the following desirable attributes:

1) Very high emission densities, for use in high-power beam-type microwave tubes.
2) Beams with low noise temperature for use in low-noise microwave tubes.
3) Instant cathode starting.
4) Long cathode life.

Barrier Material Considerations

It was decided almost at the outset that conventional insulating materials would not be the most suitable for the "tunnel" or barrier layer. There are two reasons, both having to do with the large forbidden gap

* Received by the IRE, May 31, 1960.

[1] C. A. Mead, "The tunnel-emission amplifier," PROC. IRE (Correspondence), vol. 48, pp. 359–361; March, 1960.

in insulators. For a given tunneling current density and barrier potential drop, the required barrier thickness is an inverse function of the barrier height; *i.e.*, the higher the barrier, the thinner the barrier has to be. (The barrier potential drop must be approximately equal to or greater than the work function of the surface film in order to obtain emission into the vacuum.) The uniformity and reproducibility problems of a thin film become increasingly difficult as the thickness of the film is decreased.

The second reason for deciding against conventional insulating materials is that of voltage breakdown. For a large forbidden gap and fixed barrier potential drop, the barrier thickness must be (relatively) small in order to achieve the desired tunneling current densities, as mentioned previously. The resulting high value of electric field is quite likely to cause destructive breakdown of the material. Mead reported destruction of his units at low currents.[1] This could be the result of one of two factors. First, the film thicknesses of his units could have been nonuniform. Thus some one very small area could have been producing essentially all of the emission, and attempts to increase the emission could have resulted in disruptive values of electric field over that small area. The other factor could have been the very intense values of electric field set up at the corners of his small evaporated aluminum squares, causing emission at these points and subsequent rupture upon increasing the applied potential.

At any rate, from uniformity, reproducibility, and dielectric strength considerations the writer decided essentially at the outset of his work to use a barrier material with a comparatively small forbidden gap, or in other words a semiconductor. The conductivity of the semiconductor is an important consideration, as it is desired that tunneling current should predominate over conduction current by a large factor. However, it should be recognized that bulk resistivities may be misleading when dealing with such thin films. For barrier films on the order of 50 to 500 Angstroms in intimate contact with metallic materials on both sides, the conductivity properties of the barrier material may be quite different from those of the bulk material. In effect, we are dealing with a surface phenomenon throughout the barrier, and surface states may be the important consideration rather than bulk properties.

Nevertheless, it was decided by the author that a semiconductor having high bulk resistivity would be the safest material to start with. Cuprous oxide was chosen for the initial experimental work because the calculated tunneling current, for the intended film thicknesses, greatly exceeds the conduction current calculated on the basis of bulk resistivity at room temperature.

Experimental Procedures and Results

The copper substrate was in the form of $\frac{1}{8}$ inch diameter rods. Only OFHC copper was employed, and the first step (after chemical cleaning of the surface) consisted of a vacuum-firing procedure to remove occluded gasses. The rods were then electrolytically etched in order to remove all microscopic high spots. The copper was then oxidized by several different methods, the most successful consisting of the formation first of cuprous chloride in a chloric solution and conversion at low temperature into cuprous oxide, according to the formulas:

$$Cu + Cl^- \rightarrow CuCl \quad (1)$$

$$4\,CuCl + 1/2\,O_2 \rightarrow Cu_2O + 2\,CuCl_2 \quad (2)$$

The cupric chloride product of the second reaction was dissolved out in warm water, leaving a fairly uniform and homogeneous thin film of cuprous oxide on the substrate.

The films were tested by point-contact techniques to display the current-voltage characteristics on an oscilloscope. The point-contact method has an important advantage over the evaporated film technique in that the uniformity of the coating can be subjected to direct test by probing different spots on the film. It has the obvious disadvantage, however, that the area of contact is not precisely known. Also, the contact pressure was found to be an important factor, larger pressures yielding larger tunneling currents. This is probably a result of a simple mechanical distortion of the lattice. At any rate, the pressure can be controlled in order to eliminate this variable. In addition, if the position of the Fermi level in the barrier material is known, the area of contact can be calculated, as can the film thickness, the voltage gradient, and the emission current density.

Fig. 1 shows a typical trace of the current-voltage characteristic of a point contact, taken directly from an oscilloscope. This curve would indeed appear to confirm the predominance of tunneling current over conduction current, at least for the current densities involved. If the electrical contact between the barrier layer and the substrate is presumed ohmic, then rectifying action should be in evidence for a nonohmic point contact on the cuprous oxide surface. There has been no such evidence in any of the experiments so far conducted. If the point contact on the surface is presumed ohmic, then the curve should possess a measurable slope at the origin. For all cases tested the slope is essentially zero at the origin, as in Fig. 1.

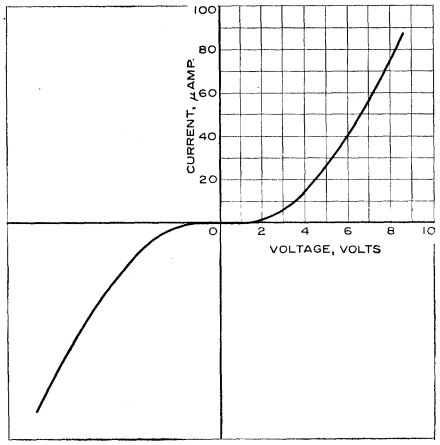

Fig. 1—Typical current-voltage tunneling characteristic of point contact on thin cuprous oxide film over a copper substrate.

Theoretical Considerations

It is believed that a good theoretical approximation to the situation being encountered can be obtained through application of the field-emission equation of Fowler and Nordheim.[2] It is only necessary to interpret the work function in the original equation as the barrier height of the semiconductor in the present application. The equation is rewritten here for convenience.

$$J = \frac{e}{2\pi h}\frac{\zeta^{1/2}}{(\zeta+\Phi)\Phi^{1/2}}E^2 \cdot \exp\left(-\frac{8}{3}\frac{\pi}{h}\sqrt{2m}\frac{\Phi^{3/2}}{E}\right) \quad (3)$$

where

J = the current density
e = the electronic charge
h = Planck's constant
ζ = the Fermi potential in the substrate
Φ = the barrier height of the semiconductor (the work function of the cold field emitter in the original usage of the equation)
E = the field strength in the semiconductor
m = the electronic mass.

The value of ζ for copper was calculated to be 7 ev from the relation

$$\zeta = \frac{h^2}{2m}\left(\frac{3n}{8\pi}\right)^{2/3} \quad (4)$$

where n is the number of free electrons per unit volume. The only unknown in (3) is then Φ, the barrier height in the semiconductor. For an assumed Φ of 0.9 volt (one-half the forbidden energy gap), (3) can be written

$$J = 2.17 \times 10^{-6}E^2 \exp\left(\frac{-57.9 \times 10^6}{E}\right). \quad (5)$$

Eq. (5) has been fitted to the experimental I-V curves of the type illustrated in Fig. 1 by matching at two arbitrary points on the curves. A comparison was then made between the experimental and theoretical curves. As shown in Fig. 2 for a typical case, the agreement is extremely close.

Typical calculated values for the film thickness and contact area from such comparisons are, respectively, 10 Angstroms

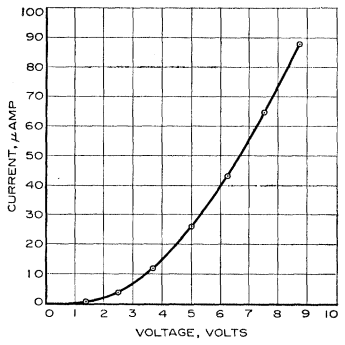

Fig. 2—Comparison between theoretical and experimental current-voltage tunneling characteristics of point contact on thin cuprous oxide film. The circles represent theoretical points plotted from (5).

[2] R. H. Fowler and L. Nordheim, "Electron emission in intense electric fields," *Proc. Roy. Soc.* (*London*) *A*, vol. 119, pp. 173–181; June, 1928.

and 2×10^{-14} cm^2. Peak calculated electric fields and current densities without dielectric rupture are typically 10^8 volts/cm and 10^{10} amp/cm^2. It is believed that the films are thicker than 10 Angstroms. If the Fermi level is actually closer to the conduction band than the assumed 0.9 volt, the calculated film thickness would be correspondingly larger. The calculated values of contact area would also be larger, and the electric fields and current densities would be correspondingly smaller.

A more desirable procedure would be an independent determination of the film thickness. This would permit an accurate evaluation of the barrier height in the semiconductor. This, in turn, would permit the evaluation of different methods of fabrication, as the Fermi level quite likely depends to a large degree on the method of preparation and the kind and concentration of impurities.

Temperature Considerations

The above measurements were all taken at room temperature. By taking measurements at different temperatures it may be possible to deduce the position of the Fermi level (and hence the barrier height) in the semiconductor film.

Temperature considerations can be expected to be important in the operation of the final finished cathode. For one thing, elevated temperatures would increase the intrinsic conductivity of the barrier layer to an intolerable level. But, more importantly, the transmission factor through the metallic surface film will certainly be a function of temperature. In fact, it may be necessary to refrigerate the cathode in order to secure sufficiently long mean free paths in the surface film.

Cold Thermionic Emission

The internal-field cathode could be operated in a space-charge-limited condition, as in the case of conventional thermionic emitters. In fact, when so operated, the internal field cathode is in every sense of the word a thermionic emitter, as only those electrons possessing sufficient thermal energy can surmount the potential barrier presented by the space-charge-formed virtual cathode and escape into the vacuum. This is true even if the cathode is refrigerated down to liquid helium temperatures. In effect, the internal field emission process produces a metallic emitting surface with an essentially zero or even negative work function, the value being controllable through the bias applied across the semiconductor film.

While ordinary high-field emitters have a comparatively high effective noise temperature[3] (owing to the absence of any virtual cathode), the internal field cathode operating under space-charge-limited conditions produces a velocity spread dependent upon the lattice temperature, just as in ordinary thermionic emitters. Therefore, a refrigerated internal field cathode should be capable of producing an electron stream in which current fluctuation noise predominates over velocity fluctuation noise. This is just the opposite of ordinary thermionic emitters. The possibilities for producing very low-noise traveling-wave tubes of otherwise conventional broad-band design are therefore quite attractive.

Conclusions

It is the author's hope that this note may contribute towards the achievement of a satisfactory internal field emitter. The potentialities offered by such a cathode appear to be rewarding enough to warrant a considerable amount of attention in the immediate future.

D. V. Geppert
Sylvania Electric Products Inc.
Mountain View, Calif.

[3] R. W. De Grasse and G. Wade, "Electron Beam Noisiness and Equivalent Thermal Temperature for High-Field Emission from a Low-Temperature Cathode," Electronics Labs., Stanford University, Stanford, Calif., Internal Memo.; March 27, 1956.

P-N Junctions Between Semiconductors Having Different Energy Gaps*

H. L. Armstrong[1] discussed the possible existence of junctions between two semiconductors of different energy gaps in 1958. He based the discussion on an earlier paper by Kroemer,[2] who had formulated a *p-n* junction in which the *p* side had a wider gap than the *n* side. Kroemer considered, in addition, the general case of an inhomogeneous semiconductor with a nonuniform bandwidth. In a germanium-silicon alloy, for instance, a change in the alloy composition might introduce a change in bandwidth in a spatial sense. Again, if the doping densities are different in two regions of a given semiconductor, the gradients of the band edges could be different for the conduction and the valence bands and the resulting quasi-electric fields could be unequal for electrons and holes.

The writer feels that these ideas can be further extended to include widely dissimilar semiconductors such as selenium and a semiconducting oxide, provided they are put together in such a manner as to form an effective junction. Reactive sputtering of a semiconducting oxide is believed to form such a junction with a suitable substrate material. An example is the junction known to exist in one type of selenium photovoltaic cell consisting of a selenium layer on which a thin layer of semiconducting cadmium oxide[3] is applied by reactive sputtering. These Se-CdO photocells, such as the Weston Type 5 Photronic® Cell, are now being produced and used in various applications. Earlier work on the photovoltaic effect in junctions between selenium and various metal oxides had been reported by Preston.[4] According to Preston, the limiting extent of the space-charge region is about 10^{-6} cm and the contact is an intimate one.

It is proposed that a junction of this type is an imperfect *p-n* junction between *p*-type selenium and the *n*-type oxide, such as represented in Fig. 1, rather than a metal semiconductor junction of the type generally described in connection with the earlier types of cells. The band gap in selenium is assumed to be 1.6 ev, as determined by Henkels[5] and Von F. Eckhart.[6] Acceptor levels are probably not more than 0.24 ev from the full band.[7]

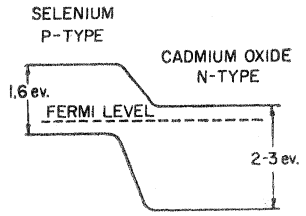

Fig. 1—The proposed Sd-CdO *p-n* junction.

The energy gap of CdO has not been determined accurately yet. An approximate estimate of 2 to 3 ev could be made on the basis of information available on ZnO. From the nature of the optical transmission through imperfect crystals, a rough value of 2 ev has been proposed.[8] Measurements made on sintered, compressed powder blocks of CdO[9] have yielded conductivities of the order of 100 ohm^{-1} cm^{-1} and carrier concentrations of the order of 10^{18}–10^{19} cm^{-3} An earlier paper by Helwig[10] on reactively sputtered CdO films gave a conductivity approximately the same as the above value; no carrier concentrations were reported.

Detailed measurements were made by the author on the conductivity and Hall constant in reactively sputtered CdO films prepared in a manner similar to those used in the typical selenium photocell. These layers exhibit a negative Hall constant, yielding a carrier concentration of approximately 10^{19} cm^{-3}. The conductivity is about 100 ohm^{-1} cm^{-1} and increases with increasing temperature. Photovoltaic junctions with selenium were also produced using highly oxidized CdO layers of much lower conductivity. These samples are undoubtedly nondegenerate. The observed conductivity is, as in the case of many other non-

* Received by the IRE, March 14, 1960.

[1] H. L. Armstrong, "On junctions between semiconductors having different energy gaps," Proc. IRE, vol. 46, pp. 1307–1308; June, 1958.

[2] H. Kroemer, "Quasi-electric and quasi-magnetic fields in nonuniform semiconductors," *RCA Rev.*, vol. 18, pp. 332–342; September, 1957.

[3] T. K. Lakshmanan, "The Weston type 5 photronic cell," *Weston Engrg. Notes*, to be published.

[4] J. S. Preston, "Constitution and mechanism of the selenium rectifier photocell," *Proc. Roy. Soc. (London) A*, vol. 202, pp. 449–466; August, 1950.

[5] H. W. Henkels, "Model of Semiconducting Selenium," presented at AIEE Winter Mtg., New York, N. Y.; January, 1954.

[6] Von F. Eckhart, "Leitfähigkeits-Messungen an Hochgereinigtem Selen," *Ann. Physik*, vol. 17, pp. 84–93; February, 1956.

[7] K. W. Plessner, "Conductivity, Hall effect and thermo-electric power of selenium single crystals," *Proc. Phys. Soc. (London) B*, vol. 64, pp. 671–681; August, 1951.

[8] N. B. Hannay, "Semiconductors," Reinhold Publishing Co., New York, N. Y., p. 590; 1959.

[9] R. W. Wright and J. A. Bastin, "The characteristic temperature and effective electron mass for conduction processes in cadmium oxide," *Proc. Phys. Soc. (London) B*, vol. 71, pp. 109–116; January, 1958.

[10] G. Helwig, "Elektrische Leitfähigkeit und Struktur aufgestäubter Kadmiumoxydschichten," *Z. Physik*, vol. 132, pp. 621–642; August, 1952.

stoichiometric oxides,[11] due to the presence of oxygen deficiency or interstitial cadmium, or both.[12] By varying the sputtering conditions wide variations in the conductivity and carrier concentration can be produced.

In the proposed p-n junction between nondegenerate CdO and Se, Fig. 1, the energy gaps are assumed to be different and the quasielectric field for electron flow differs from that for hole flow. The general equations for current flow under dark conditions are, for such a junction,

$$J_h = e\mu_h pE^{(h)} - eD_h\nabla p$$
$$J_e = e\mu_e nE^{(e)} + eD_e\nabla n$$

where J is the current density, D the diffusion constant, μ the mobility and n and p the electron and hole densities, respectively. The subscripts or superscripts e and h refer, respectively, to electrons and holes.

It is interesting to note that Yamaguchi[12] had postulated that in the case of a blocking layer rectifier, the rectifying action existed at the junction between Se and CdSe and not at the CdSe-Cd junction. CdSe is well known to be n-type. More recently, Yashukova[13] has pointed out that a p-n junction may be supposed to exist between Se and CdSe. Furthermore, a simplified scheme with equal energy gaps on the p and n sides and with a barrier film in between has been given by Dietzel, Gorlich and Krohs[14] for a special type of selenium photovoltaic cell. The present scheme is considered to be an extension of these ideas.

Further work on the semiconducting properties of CdO is continuing. A more detailed examination of this type of p-n junction with unequal gaps is also being made.

T. K. Lakshmanan
Weston Div.
Daystrom, Inc.
Newark, N. J.

[11] E. J. W. Verwey and F. A. Kröger, "New views on oxidic semiconductors and zinc-sulphide phosphors," *Philips Tech. Rev.*, vol. 13, pp. 90–95; October, 1951.
[12] J. Yamaguchi, "On the blocking layer of selenium rectifier (II)," *J. Phys. Soc. Japan*, vol. 10, pp. 234–236; March, 1955.
[13] I. M. Yashukova, "Electrical Conductivity of Polycrystalline CdSe," *Soviet Phys.* (Solid-State), vol. 1, p. 349; March, 1959.
[14] G. Dietzel, P. Gorlich, and A. Krohs," Über Selenphotoelemente," in "Jenaer Jahrbuch," VEB Carl Zeiss, Jena, Ger., vol. 1, pp. 203–277; 1958.

An Optimal Discrete Stochastic Process Servomechanism*

In an article to be published elsewhere,[1] a complete optimal class of servos is derived which provides maximal smoothing in a certain novel sense for discrete stochastic processes. The present note represents an extension of Mills' theorem to indicate a particular member of the optimal class which, in addition to assuring maximal smoothing in Mills' sense, also provides quickest response and zero average error.

A brief review of Mills' theory is necessary in order to appreciate the import of and constraint upon the present extension. Thus Mills considers a discrete servo-stochastic process defined to be a sequence of random variables of the form

$$P = (e_1, c_1, n_1, e_2, c_2, n_2, \cdots,) \quad (1)$$

where

e_t is interpreted as an "error" in an operation at the beginning of time period t,
c_t is a "correction" made in the operation at the beginning of period t, but with prior knowledge of e_t,
n_t is the "noise" entering the operation during period t.

The process P, in conjunction with a sequence of numbers representing the "initial conditions," is characterized by the following properties, for $t=0, 1, 2, \cdots$,

$$e_{t+1} = e_t + c_t + n_t \quad (2)$$
$$c_{t+1} = S(\cdots, n_{t-1}, e_t, c_t, n_t) \quad (3)$$
$$\text{Prob}\ (n_t \leq x) = N(x) \quad (4)$$

where S is an arbitrary function and N is an arbitrary distribution.

Eq. (2) represents a conservation of error in the operation (holding with probability 1); (3) specifies a "servo" or "decision policy" S (also holding with probability 1); and (4) describes the noise, which is taken to be identically and independently distributed period by period. The objective of Mills' paper is to determine that class of servos, that is, that class of functions, S, which are optimal in a certain sense. The sense in which they are optimal is related to an "uncertainty principle" for servo-stochastic processes, derived by Mills, namely, that for any servo

$$k_e \geq \frac{1}{2}\left(k_c + \frac{1}{k_c}\right), \quad (5)$$

or, in another form,

$$k_e k_c \geq \tfrac{1}{2}(1 + k_c^2) \geq \tfrac{1}{2}, \quad (6)$$

wherein k_e and k_c are respectively defined by

$$k_e = \sigma_e/\sigma_n, \qquad k_c = \sigma_c/\sigma_n, \quad (7)$$

the sigmas being variances, and it being assumed that $\sigma_n^2 > 0$. The ratios k_e and k_c, Mills calls the "error to noise ratio" and the "correction to noise ratio;" k_e gives a measure of "how well the servo is doing" and k_c gives a measure of "how hard the servo is working." Eqs. (5) and (6) demonstrate that both these ratios cannot simultaneously be decreased indefinitely by better servo design. Mills terms the relations (5) and (6) the "smoothing capacity" of servos in discrete servo-stochastic processes.

Mills limits his analysis to stable processes, that is, to those for which all first and second-order statistical moments approach definite limits in time, *e.g.*,

$$\bar{e} = \lim_{t\to\infty} \bar{e}_t, \qquad \bar{c} = \lim_{t\to\infty} \bar{c}_t, \qquad \bar{n} = \bar{n}_t,$$
$$\sigma_e^2 = \lim_{t\to\infty} \sigma_e^2(t), \qquad \text{etc.} \quad (8)$$

[where $\bar{e}_t = E(e_t)$, $\bar{c}_t = E(c_t)$, $\bar{n}_t = E(n_t)$, and E denotes the expectation or mean value].

Mills then formulates a complete optimal class of servos which achieves the equation form of the inequality of (5). These optimal servos turn out to be linear, namely, of the form

$$c_t = -\alpha(e_t - \beta) \quad (9)$$

where $0 < \alpha \leq 1$, and β is arbitrary.

As Mills states, "That so simple a class of policies is complete and optimal seems quite fortuitous considering the fact that they are in competition with all possible servos, nonlinear, discontinuous, or what have you." Eq. (9) is Mills' optimal class of servos; that is, (9) gives the form of the function S of (3) which is optimal in the sense that the uncertainty principle of (5) is minimized. Mills also demonstrates that the same class is also optimal for the case in which there are information time delays and/or servomechanical response times. Thus, with a composite time delay of T periods, the "uncertainty principle" of (5) is amended by squaring the expression and then adding the term $+T$ on the right-hand side, but the optimal class of servos given by (9) remains optimal without alteration.

The extension of Mills' theorem to include optimization with respect to response time and average error is easily gained as follows.

In the course of his derivation, Mills exhibits a formula for the limit average error,

$$\bar{e} = \frac{\bar{n}}{\alpha} + \beta. \quad (10)$$

Now the conditional expectation value of the error on the $t+1$ period, given the error on the previous period, is given by

$$\begin{aligned} E(e_{t+1}/e_t) &= E(e_t + c_t + n_t/e_t) \\ &= E(e_t(1-\alpha) + \alpha\beta + n_t/e_t) \\ &= (1-\alpha)e_t + \alpha\beta + \bar{n} \\ &= (1-\alpha)e_t + \alpha\bar{e}. \end{aligned} \quad (11)$$

In the evaluation of the conditional expectation, we have employed the expression for the optimal-smoothing servo class, given by (9). If in (11) we choose α to be equal to 1, then the expected error is no longer conditional, but is simply given by the average error independent of the previous history of the servo. Returning to (10), now with $\alpha = 1$, we see that minimal average error, namely 0 error, is gained by choosing the arbitrary constant β to be equal to the negative of the average noise. Thus letting $\alpha = 1$, and $\beta = -\bar{n}$, insertion in (9) yields

$$c_t = -(e_t + \bar{n}). \quad (12)$$

This simple expression represents the optimal servo which, providing maximal smoothing, assures quickest response, and zero average error. It is quickest in the sense that given some initial nonaverage error, the servo "assures" return to the mean error in the shortest number of periods possible, namely 1. Any other choice of α would lead to a servo which would approach the mean error value only in the limit.

The servo represented by (12) is the one which an engineer is first tempted to apply in any error correction servo system. It states that the correction to be applied is the negative of the error resulting from the previous step, plus the negative of the expected noise. Stated another way, if one has

* Received by the IRE, February 12, 1960.
[1] H. D. Mills, "Smoothing in discrete servo-stochastic processes," submitted for publication in the *J. Soc. Indus. and Appl. Mechanics.*

an error e_t, and one knows that the average noise is $\bar{n}$, then the "simple-minded" solution would be to make a correction given by the negative of the sum of the two errors. The extraordinary fact is that this "simple-minded" design is optimal, in that it provides maximum smoothing, quickest response, and zero average error.

GEORGE C. SPONSLER
Hoffman Electronics Corp.
Science Center
Santa Barbara, Calif.

On Stabilizing the Gain of Varactor Amplifiers*

A number of regenerative varactor amplifiers have been tested with a view to their use as low-noise preamplifiers in certain radioastronomical observations where a gain constancy of the order of one part in a thousand is required. This note is an account of experience with the stabilization of the so-called "degenerate" amplifier where $f_p = 2f_s$.

The power gain of a regenerative varactor amplifier is a sensitive function of the impedances presented to the varactor, and of the pump power level. For many situations, adequate impedance stability can be achieved by using rigid structures and firm connections, avoiding sliding contacts in the tuning systems, paying close attention to serving the cables and connectors, and using stable pump frequencies. Stabilizing the pump power level at the varactor requires equal care in the construction of the pump oscillator and the interconnecting circuits. But despite these precautions, the experimental amplifiers, using both fixed and self-bias, showed unacceptable gain variations which were traced to residual changes in the pump power level.

During the initial measurements on a 2000-mc degenerate amplifier using a germanium diode (Hughes type HPA 2810) and a low resistance bias circuit, it was noticed that the gain tended to become independent of the pump power level when the amplitude of the pump voltage was close to the value of the bias voltage. The degree of saturation observed depended upon the tuning of the signal and pump circuits. This behavior is illustrated by curves *a* and *b* of Fig. 1. With the adjustment of curve *b*, which placed the peak of the gain curve at a point where the net varactor dc current was zero (see Fig. 1, curve *c*), the gain remained constant to within ±1 per cent over a period of one hour. This saturation effect appears to be caused by a slight increase in the varactor losses and to the dependence of the mean varactor capacitance on the pump level, resulting in a change in both damping and tuning of the signal and pump circuits. No such tendency to saturate was observed with self-bias.

A considerable further improvement in gain stability was achieved by using the

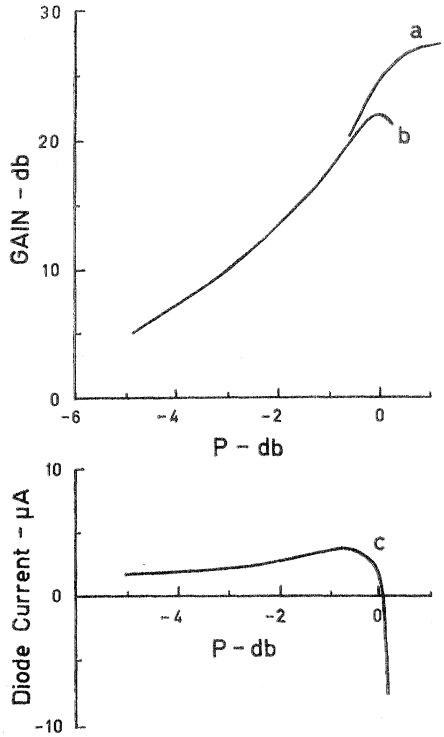

Fig. 1—Variation of insertion gain and dc varactor current as functions of the relative available pump power, *P*. Results for Hughes HPA2810 germanium varactor at 2000 mc with fixed bias of 2.7 volts.

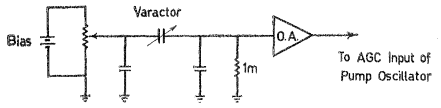

Fig. 2—DC circuit of pump stabilizer.

varactor dc current to control the pump level. The circuit of Fig. 2 was utilized to control the pump power so that operation was always at the crossover point "X" of curve *c* of Fig. 1.[1]

In Fig. 2, "O.A." is a high gain, chopper stabilized, dc operational amplifier with an equivalent input noise current less than a millimicroampere (Philbrick USA series units). Because of the steepness of the rectified varactor current characteristic, and the precautions discussed earlier, it has been possible to achieve an excellent gain stability. On the laboratory bench at gain settings of 20–25 db, the gain of a 400-mc amplifier was found to be more stable than that of the test receiver used, the measurements merely indicating that the instability was of the order of, or less than, one part in a thousand over periods of half an hour or more. Further, it has been possible to make precise measurements of excess noise, gain, and bandwidth, when operating at gains as high as 40 db. Thus it appears that gain fluctuations caused by pump variations are now relatively unimportant compared to those caused by impedance changes.

The stabilization scheme described above would appear to be susceptible to changes in the varactor currents caused by ambient temperature variations. In the laboratory no significant temperature sensitivity has been observed.

The rectified pump current will increase the noise generated in the amplifier beyond the value expected from the circuit and varactor losses. At 2400 mc and operating at the crossover point, the noise temperature has been observed to increase by about ten per cent from its minimum value for a *maximum rectified reverse current* of one μa.

This work has been carried out under the auspices of the Netherlands Foundation for Radio Astronomy, supported by the Netherlands Organization for Pure Research (Z.W.O.). One of the authors (Robinson) has been seconded from the Radiophysics Laboratory of C.S.I.R.O. (Australia).

B. J. ROBINSON
C. L. SEEGER
K. J. VAN DAMME
J. T. DE JAGER
The Leiden Observatory
Leiden, The Netherlands

A Conference on the Propagation of ELF Electromagnetic Waves*

On January 26, 1960, a conference was held at the Central Radio Propagation Laboratories (CRPL) in Boulder, Colo., which was devoted mainly to the subject of radiowave propagation of extremely low frequencies (ELF). The frequency range (less than about 3 kc) is well below those currently used in communications. Lightning discharges, however, produce considerable energy in this range, and the radiated fields have been used for studying the nature of lightning phenomena for many years at frequencies as low as 10 cps. Other natural sources of both a terrestrial and an extra-terrestrial nature also radiate electromagnetic energy in this frequency range, but usually to a lesser extent than lightning.

Since ELF signals have been observed to propagate with very low attenuation, it has been suggested from time to time that they would be useful for communications on a world-wide scale. Furthermore, because of certain magneto-ionic phenomena, these waves may penetrate the ionosphere and enable communication with space vehicles. This is particularly so in the vicinity of 3 kc where a "window" in the ionosphere appears to exist. Another aspect of ELF waves is that the wavelength is extremely large (3000 km at 100 cps) and consequently, the signals may easily be diffracted around planetary objects. Furthermore, such signals penetrate with relatively small loss into conducting media such as rocks and soil. In fact, frequencies in this range have been used for many years in geophysical exploration.

The topics discussed at the conference were divided into two sessions. The first dealt with observed characteristics of natural ELF fields and was moderated by J. R. Wait. The second dealt with the theory of radiation and propagation of these waves and was moderated by A. D. Watt. A very

* Received by the IRE, May 13, 1960.

[1] This general method of stabilization has been used before in the design of ultra-stable conventional crystal mixers.

* Received by the IRE, February 23, 1960.

sketchy description of the individual presentations is presented here.

E. T. Pierce of Avco Corporation, Wilmington, Mass. gave an introductory paper on the nature of the waveforms of signals radiated from lightning discharges. He indicated that the characteristics of the "slow tail" portion of the waveform enabled electron densities and collision frequencies to be deduced for the lower edge of the ionosphere E region.

George Garland of the University of Alberta, Edmonton, Can., then presented a comprehensive paper on the nature of fluctuations of the earth's magnetic field. Particular attention was given to the basis of the magneto-telluric method of investigating the earth's crust. Essentially, the idea is to compare the tangential electric and magnetic field variations on the surface of the earth. The variation of the ratio of the frequency spectra of these fields is related to the conductivity of the earth's crust at depths of the order of kilometers.

W. Campbell of the University of Alaska, College, discussed the diurnal and seasonal variations of geomagnetic fluctuations. He concluded that for frequencies above about 2 cps the sources of the fields were primarily from lightning discharges, while below this frequency the field variations must be attributed to solar effects. Further papers on geomagnetic fluctuations were given by P. A. Goldberg of RAND Corporation, Santa Monica, Calif., and E. Maple of Air Force Cambridge Research Center, Cambridge, Mass. Both these authors confirmed the idea that magnetic energy in the audio-frequency range could be attributed almost solely to lightning discharges.

A. D. Watt and E. L. Maxwell of CRPL discussed the physical phenomena involved in cloud-to-ground lightning discharges, and the respective role of the static, induction, and radiation fields. The radiation field was shown to vary directly with frequency below about 6 kc, and observed spectral characteristics which depart from this law were satisfactorily explained.

A. G. Jean and W. L. Taylor of CRPL briefly described their experimental facilities for measuring the waveforms of atmospherics in this ELF range. The significant feature of the scheme is that simultaneous recordings are made of the same atmospheric at widely separated stations.

E. L. Tepley presented an extensive summary of the activities of the Institute of Geophysics at the University of California at Los Angeles. This included a statistical study of the characteristics of "atmospheric waveforms" using a large number of samples. Data on attenuation rates of ELF signals were also discussed. For example, at 100 cps, these are of the order of 1 db per 1000 km of path length.

In the first paper of the second session, J. R. Wait of CRPL gave a theoretical treatment of mode theory with special reference to ELF. The effect of earth curvature and the earth's magnetic field were included in the analysis. Particular attention was focused on the behavior of the electric and magnetic fields at distances from the source which were comparable to the wavelength. In the following paper, R. A. Helliwell of Stanford University, Stanford, Calif., mentioned certain peculiar characteristics of the whistler sonograms which indicate that whistlers sometimes contained appreciable energy at ELF.

W. L. Anderson of the University of New Mexico, Albuquerque, presented a theoretical discussion of the dispersion of electromagnetic pulses propagating in conducting media. Certain recommendations were made concerning the optimum pulse shape for signalling.

The transmission between two insulated loop antennas immersed in a conducting half-space was evaluated by H. A. Wheeler of Wheeler Laboratories, Great Neck, N. Y. He used a very straightforward method which made use of the reciprocity theorem and the known solution of the receiving antenna problem. In a sequel to this paper, L. Rawls of Developmental Engineering Company, Norwalk, Conn., discussed the engineering design of buried antennas. K. A. Norton of CRPL then emphasized the advantages of the system-loss concept in presenting radiation and propagation data at ELF.

R. K. Moore and R. H. Williams of the University of New Mexico, Albuquerque, outlined a theoretical treatment of the horizontal electric antenna immersed in a conducting half-space. Essentially, the problem is a generalization of the Sommerfeld problem of a dipole on the surface of the half-space. They also considered the impedance of the antenna, using an approximate method which has its roots in transmission line theory. C. H. Harrison, Jr. of Sandia Corporation, Albuquerque, N. M., then presented a full treatment of the finite cylindrical antenna immersed in a conducting medium of infinite extent. The King-Middleton method of iteration for antennas in air was modified for the case of dissipative media. This was followed by R. S. Macmillan of the University of Southern California, Los Angeles, who gave an account of investigations of power-line antennas. Essentially, the idea is to excite a section of power line which acts as a horizontal center-fed dipole. The pattern has a maximum looking straight up and thus is very suitable for ionospheric investigations.

Finally, G. V. Keller and F. Frischknecht of the U. S. Geological Survey, Denver, Colo., presented a paper on their electrical investigations of glaciers and ice sheets using audio frequencies. The energy was coupled to the medium by both electrodes and loops. Using such schemes, it was possible to outline the cross sections of the Athabaska glacier in Alberta, Can.

Papers from the conference will be published in early issues of the *Journal of Research* of the National Bureau of Standards, Section D (Radio Propagation). An edited transcript of the oral discussions following the papers is to be available.

A Note on Nomenclature

It is suggested by A. D. Watt and the author that the following designations be employed for these extra low frequencies.

VLF (very low frequency),	3 to 30 kc;
ELF (extremely low frequency),	1.0 to 3000 cps.

J. R. Wait
National Bureau of Standards
Boulder, Colo.

WWV and WWVH Standard Frequency and Time Transmissions*

The frequencies of the National Bureau of Standards radio stations WWV and WWVH are kept in agreement with respect to each other and have been maintained as constant as possible with respect to an improved United States Frequency Standard (USFS) since December 1, 1957.

The nominal broadcast frequencies should, for the purpose of highly accurate scientific measurements, or of establishing high uniformity among frequencies, or for removing unavoidable variations in the broadcast frequencies, be corrected to the value of the USFS, as indicated in the table below.

The characteristics of the USFS, and its relation to time scales such as ET and UT2, have been described in a previous issue,[1] to which the reader is referred for a complete discussion.

The WWV and WWVH time signals are also kept in agreement with each other. Also they are locked to the nominal frequency of the transmissions and consequently may depart continuously from UT2. Corrections are determined and published by the U. S. Naval Observatory. The broadcast signals are maintained in close agreement with UT2 by properly offsetting the broadcast frequency from the USFS at the beginning of each year when necessary. This new system was commenced on January 1, 1960. The last time adjustment was a retardation adjustment of 0.02 s on December 16, 1959.

WWV Frequency
With Respect to U. S. Frequency Standard

1960 June 1600 UT	Parts in 10^{10}†
1	−144
2	−144
3	−144
4	−144
5	−144
6	−145
7	−145
8	−146
9	−146
10	−146
11	−146
12	−146
13	−147
14	−147
15	−147
16	−146
17	−146
18	−146
19	−146
20	−147
21	−147
22	−147
23	−147
24	−147
25	−147
26	−147
27	−147
28	−146
29‡	−146
30	−148

† A minus sign indicates that the broadcast frequency was low.

‡ Method of averaging is such that an adjustment of frequency of the control oscillator appears on the day it is made. The frequency was decreased 3×10^{-10} on June 29.

National Bureau of Standards
Boulder, Colo.

* Received by the IRE, July 25, 1960.

[1] "United States National Standards of Time and Frequency," Proc. IRE, vol. 48, pp. 105–106; January, 1960.

Energy Fluxes from the Cyclotron Radiation Model of VLF Radio Emission*

Several authors[1,2] have suggested that certain natural audio-frequency electromagnetic background radiations, notably dawn chorus, are due to cyclotron radiation from protons incident on the earth's exosphere. The principal success of this theory is that with the Doppler and ionospheric dispersion effects taken into account, the theory nicely predicts the frequency *vs* time characteristics of the observed signals. The purpose of this note is to point out that the cyclotron theory, at least in its simple form, does not seem to account for the observed strength of the radiation. A crude calculation suffices to show a discrepancy.

We consider that the radiation comes from a spherical shell of thickness d centered around the earth at a mean altitude h above the earth's surface. The streams of incoming protons are described by a number density n and a particle velocity v. The expression for the radiated power passing through a horizontal unit area at the earth's surface involves the inverse-square spreading factor, the angular distribution and polarization of each elementary radiator, the magnetic field strength B, and the absorption and anisotropic propagation properties of the medium. This expression is difficult to evaluate. However, if we assume isotropic radiation from each volume element and phase coherence of all elementary radiators, some geometrical manipulations show that

$$P \approx nSd,$$

where P is the power incident on a horizontal unit area and S is the total power radiated by a charged particle moving (adiabatically) in a circular orbit.

The "enhanced" solar wind, characteristic of the active solar conditions under which dawn chorus is most frequently observed, may have a particle density of 10^4 to 10^5 protons per cm^3 and a particle velocity of 1500 km/sec. These parameters suggest that the particle flux will penetrate the geomagnetic field to a distance of about 1.5 earth radii.[3] Therefore, we postulate the radiating layer to be at an altitude of about 3500 km above the earth's surface. The effective layer thickness d can be estimated by computing the radial distance over which the magnetic field changes sufficiently to account for the observed bandwidth of the signal.[4] MacArthur[1] has shown that the true radiated frequency is inversely proportional to B. Then if ν is the radiated frequency, $\Delta\nu$ is the signal bandwidth, and ΔB the corresponding change in magnetic field, we have

$$\Delta B = B\left|\Delta\nu/\nu\right|.$$

If we represent the earth's field by a dipole of moment $p=8\times10^{10}$ gauss-km^3, we may write $B=pr^{-3}(4-3\sin^2\theta)^{\frac{1}{2}}$. Then,

$$d \approx \Delta B\left(\frac{\partial B}{\partial r}\right)^{-1} = \frac{r}{3}\left(\frac{\Delta\nu}{\nu}\right).$$

The quantity $\Delta\nu/\nu$ does not exceed 0.2,[5] and we conclude that $d\approx700$ km. The quantity S may be written in mks units as

$$S = \mu\frac{e^4B^2v^2}{6\pi cm_p^2}.$$

At an altitude of 3500 km and middle geomagnetic latitudes ($\theta\approx45°$), $B=0.12$ gauss. If we take $v=1500$ km/sec, and note that in this part of the earth's exosphere the local velocity of light is about 1/100 the free space value,[2] we find $S\approx2\times10^{-33}$ watts. Taking a particle density of 10^5 per cm^3, the energy flux density estimate becomes

$$P \approx 1.5\times10^{-16}\ \text{watts/m}^2.$$

Sferics, short electromagnetic pulses coming from lightning discharges, are by far the most energetic source of natural electromatic noise in the audio-frequency region. This sferic background level determines the ultimate detectability of signals from other sources. The sferic power spectrum shows a minimum in the neighborhood of 2 to 3 kc, and this minimum value will be used in making the following estimate of marginally detectable signal strengths. Although the sferic spectrum is highly variable, a reasonable estimate[6] for the mean field strength is $b\approx10^{-9}$ gauss/cps. This value leads to a background energy flux density in a 500 cps bandwidth of about 1.5×10^{-8} watt/m^2. Let us assume that b has been overestimated by a factor of 10, and further assume that a continuous signal of 1/1000 the flux density of the background can just be detected. This minimum detectable energy flux density is then

$$P(\text{min}) \approx 1.5\times10^{-13}\ \text{watts/m}^2.$$

The dawn chorus fluxes observed must therefore equal or exceed this value. Hence it appears that the proton cyclotron radiation model fails by about a factor of 10^3 to account for the strength of the emissions.

In view of the crudity of the calculation, a factor of 10^3 is not conclusive. However, the isotropic radiating layer approximation probably overestimates the true situation in which focusing and absorption effects are included, and the minimum detectable signal flux has been estimated very conservatively. The basic difficulty with the cyclotron model is that cyclotron radiation is a very inefficient process for converting kinetic energy at audio frequencies. Also it is difficult to visualize how the necessary phase coherence can be obtained over a large volume of elementary radiators. The theory of Gallet,[7] in which the energy conversion process is similar to that in a traveling-wave tube, appears to offer the possibility of substantially better conversion efficiency. Furthermore, the necessary condition of Gallet's mechanism (that the particle velocities equal the local phase velocity of light) seems quite likely to be fulfilled at some point in the exosphere.

The author is indebted to Dr. J. W. MacArthur for a critical reading of the manuscript.

R. A. Santirocco
Stromberg-Carlson Division
of General Dynamics Corp.
Rochester, N. Y.

* Received by the IRE, February 18, 1960.

[1] J. W. MacArthur, "Theory of the very low-frequency radio emissions from the earth's exosphere," *Phys. Rev. Letters*, vol. 2, pp. 491–492; June 15, 1959.

[2] W. B. Murcray and J. H. Pope, "Doppler-shifted cyclotron frequency radiation from protons in the exosphere," *Phys. Rev. Letters*, vol. 4, pp. 5–6; January 1, 1960.

[3] E. N. Parker, "Auroral phenomena," PROC. IRE, vol. 47, pp. 239–244; February, 1959.

[4] We do not wish to imply that the magnetic field gradient is the only cause of broadening.

[5] See for example the frequency-time plots in footnotes 2 and 7.

[6] J. B. Wilcox and E. Maple, "Audio-Frequency Fluctuations of the Geomagnetic Field," U. S. Naval Ord. Lab. Navord Rept. 4009; July 9, 1957.

[7] R. M. Gallet, "The very low-frequency emissions generated in the earth's exosphere," PROC. IRE, vol. 47, pp. 211–231; February, 1959.

A Receiver for Observation of VLF Noise from the Outer Atmosphere*

Although high-frequency radio outbursts from the solar corona have been studied intensively over the past decade, it is only recently that much attention has been paid to the analogous radiations at kilocycle frequencies which are generated in the outer atmosphere of the earth, and there have been no reports of any extended series of observations which would compare with those made of solar radio emissions.

Nevertheless, observations of radio noise from the outer atmosphere provide a useful new technique for studying the processes responsible for auroras. It has been shown, for example, that charged particles traversing the plasma of the outer atmosphere will generate Cerenkov-like radiation at frequencies between about 1 kc and 1 mc.[1,2] As a result, it is likely that there is a steady background of radio noise in this frequency range because of the Van Allen particles, superimposed on which are much more intense bursts of noise caused by the passage of auroral particles through the atmosphere. Recent observations of the geographical pattern for illumination of a small region of the earth of radiation in the kilocycle band have suggested strongly that it is both patchy and sporadic.[2] It now seems likely that the study of the worldwide pattern will provide, for the first time, a map of the disturbed regions of the outer atmosphere which are the sources of auroral particles. It is therefore of considerable importance that observations be made at many places and to stimulate interest in such observations, a suitable receiver is described in this paper.

One of the principal reasons for the absence of previous observations of noise bursts at kilocycle frequencies has been the difficulty of recording them in the presence of the relatively much stronger interference from electric mains and from atmospherics

* Received by the IRE, March 4, 1960.

[1] G. R. A. Ellis, "Low frequency radio emission from aurorae," *J. Atmos. Terr. Phys.*, vol. 10, pp. 302–306; 1957.

[2] V. Ia. Eidman, "The radiation from an electron moving in a magnetoactive plasma," *J. Exptl. Theoret. Phys. (U.S.S.R.)*, vol. 34, pp. 131–138; January, 1958.
V. Ia. Eidman, "Soviet physics," *J. Exptl. Theoret. Phys. (U.S.S.R.)*, vol. 7, pp. 91–95; July, 1958.

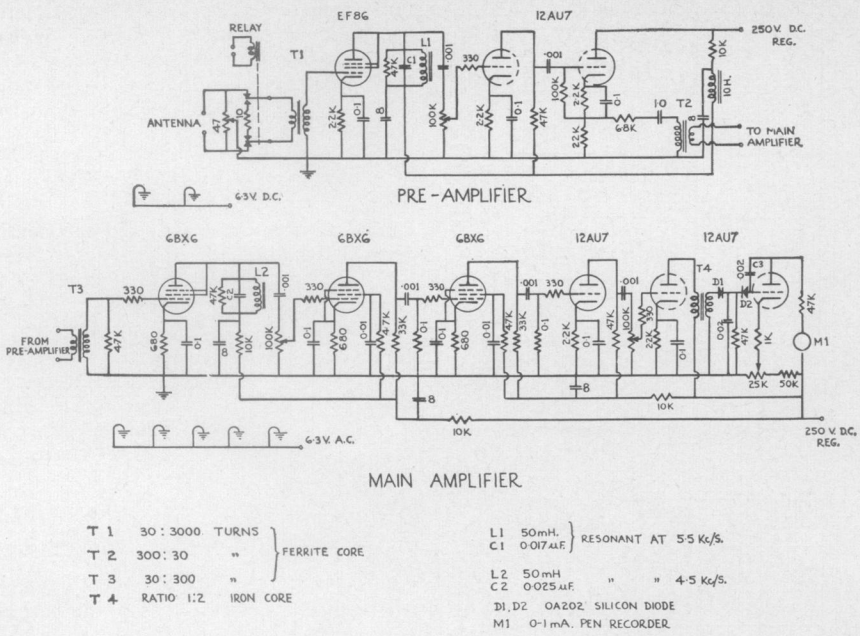

Fig. 1.

in the same frequency band. Although many attempts have been made at places remote from electrical supply systems the interference from atmospherics has still caused difficulties. Yet the wanted noise signal is usually bandwidth-limited white noise while the interference is impulsive, taking the form of intermittent short pulses, which last, for atmospherics, a fraction of a second, and, for mains, a few thousandths of a second recurring at half the mains period. Well-known techniques are available for improving signal-to-interference ratio in situations like this. Here a minimum reading recorder is used and has been found satisfactory. With this, discrimination against impulsive interference of the order of 30 db can be obtained without difficulty. This makes it possible to record easily noise bursts at 5 kc at geomagnetic latitudes greater than about 40°. This frequency has been chosen because it coincides both with a trough in the atmospherics spectrum and a peak in the VLF noise spectrum.

In its main details, the receiver follows practice standard for observations of whistling atmospherics.[3] The antenna is a four-turn vertical loop, 100 square meters in area and orientated in a north-south direction, which is connected to the preamplifier through a transformer with a turns ratio of 1:100. Because of the extremely small radiation resistance of the antenna, it is not feasible to match it to the input stage. To reduce mains interference, the preamplifier and antenna are 100 meters from the building housing the main amplifier and recording equipment. Signals in the frequency band from 4–6 kc are amplified in the main amplifier and, after rectification, are averaged in an RC circuit with a time constant of one millisecond. The dc output is then amplified further and applied to the minimum reading circuit (Fig. 1). When a positive-going pulse appears at the cathode or the detector D1, the impedance of diode D2 is very large and, together with the capacitor C3, presents a time constant of 30 seconds to the incoming signal. Negative-going pulses, on the other hand, cause the diode to conduct, lowering its impedance and giving a time constant of two milliseconds. The output of the minimum reading circuit is proportional to the average level of the continuous background noise, providing there are intervals of a few thousandths of a second in between the interfering impulses.

Receivers similar to this have been operated during the past twelve months at Camden (near Sydney), Hobart and Adelaide.[4] Apart from operating them away from the vicinity of electrical machinery, no special precautions have been taken to select noise-free sites. It has been found that the amplitude of the VLF noise increases with geomagnetic latitude, being about twice as great as Hobart [51° geomagnetic latitude as Camden (42°)]. The gain of the Camden receiver is normally set so that 0.65-μv input to the aerial terminals from a signal generator produces full scale deflection of the pen recorder at 5 kc. This corresponds to a radiation field strength of 0.36 $\mu v/m(c/s)^{-1/2}$. The recorded level of background noise interference is usually about 0.01 $\mu v/m^{-1}(c/s)^{-1/2}$, arising to double this at night when atmospherics become stronger The field strength of VLF noise bursts varies between 0.03 and 0.2 μv/m at Camden. The receiver sensitivity for signal equal to first-stage noise is 0.003 $\mu v/m^{-1}(c/s)^{-1/2}$.

One of the most important aspects of setting up the receiver is to ensure that strong impulsive signals from atmospherics are not limited unsymmetrically in the final amplifying stages. If this occurs, spurious low-frequency signals can be generated by the shift of bias levels. Adjusting the bias of the final stages will normally correct this condition.

G. R. A. Ellis
Upper Atmosphere Section
Commonwealth Sci. and
Industrial Res. Organization
Camden, N. S. W., Australia

[3] L. R. O. Storey, "An Equipment for Recording Whistlers Automatically," Defence Res. Telecommun. Est., Ontario, Can., Project Rept. No. 23-4-3; 1956.

[4] G. R. A. Ellis, "Low-frequency eiectromagnetic radiation associated with magnetic dlsturbances," *Planet. Space Sci.*, vol. 1, pp. 253–258; September, 1959.

An X-Band Parametric Amplifier Using a Silver-Bonded Diode*

The authors had previously reported that a silver-bonded germanium diode was suitable for a parametric amplifier diode, and that low-noise parametric amplifications were obtained by the use of these diodes at 4 and 6 kmc.[1,2] Recently, the authors have succeeded in getting the low-noise parametric amplification up to 11 kmc by utilizing the same type of diode as is assembled at the Electrical Communication Laboratory of the Nippon Telegraph and Telephone Public Corporation, Tokyo, Japan. This paper presents the results of such an amplifier.

The silver-bonded diode was constructed in the manner of the so-called "wafer type," that is to say, an *N*-type germanium piece was mounted at one broad side of a rectangular waveguide of a metal wafer, which was inserted transversely through the gap of the waveguide holder as shown in Fig. 1. A silver-gallium whisker of 100 microns in diameter inserted from the opposite side of the waveguide was in contact with the wafer at its tip. An electrical forming process was used by discharging current from a condenser through the contact point. The typical voltage-current characteristic of the diode is shown in Fig. 2. The barrier capacitance at breakdown voltage, the series resistance and the cut-off frequency of the diode are about 0.1 pF, 5 ohms and 300 kmc, respectively.

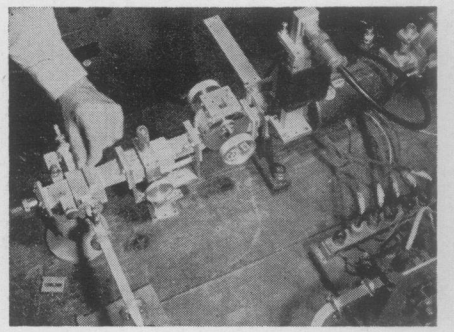

Fig. 1—Photograph of the amplifier.

* Received by the IRE, February 9, 1960.

[1] B. Oguchi, S. Kita, N. Inage and T. Okajima, "Microwave parametric amplifier by means of germanium diode," PROC. IRE, vol. 47, pp. 77–78; January, 1959.

[2] S. Kita, K. Sugiyama and T. Okajima, "Properties of silver bonded diode for parametric amplifier," ELECTRON DEVICES Meeting, Washington, D. C.; October 29–31, 1959.

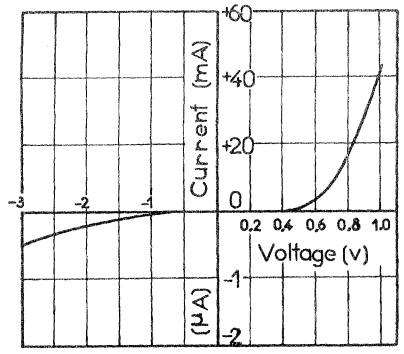

Fig. 2—Voltage-current characteristic of the silver-bonded diode.

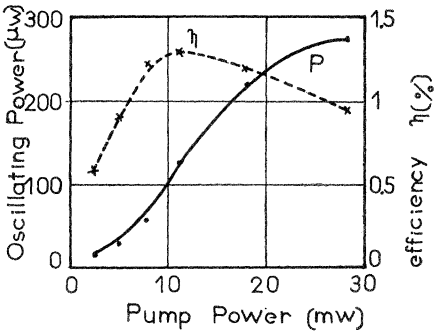

Fig. 3—Oscillation characteristics.

As the amplifier, a cross-type waveguide, a three-stub tuner of the K band and a slide-screw tuner of the X band were used. Two waveguides of the X and K bands were connected crosswise at both H planes.

The height of the X-band waveguide was tapered to the same height of the K-band waveguide. The diode was located near the cross point.

The pump power at a frequency of 23 kmc was supplied from a 2K33 klystron through a K-band isolator. An oscillation at one-half the pump frequency was produced by adjusting the three-stub tuner, the waveguide piston and the slide-screw tuner. The measured oscillating power vs pump power curve is shown in Fig. 3. The best efficiency was about 1.2 per cent at 10 mw pump power. The minimum required pump power for oscillation was about 1 mw.

As the slide-screw tuner was adjusted a little from the point of the oscillation, the oscillation stopped and the signal of almost one-half the pump frequency could be amplified at this condition for the nondegenerate-type amplification.

A typical amplification, bandwidth and noise figure vs bias voltage characteristics of the amplifier are shown in Fig. 4. In this case, the center frequency of the amplified signal is 11,440 mc, the pump frequency is 23,000 mc, and its power about 4 mw.

The noise figure was measured by using an X-band signal generator and a receiver. As the result, the minimum value of about 6.5 db was obtained for the single sideband operation. By increasing the pump power, the gain-band product of the amplifier increased, as shown in Fig. 5, and a gain of 15 db with a 50-mc bandwidth was produced at about 10 mw pump power.

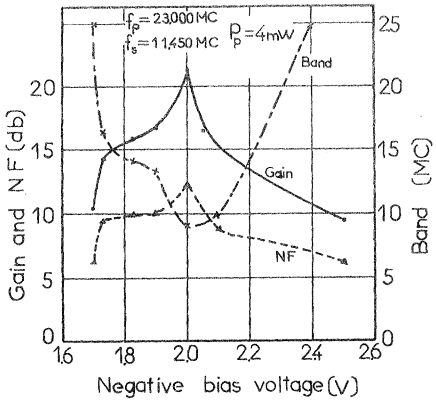

Fig. 4—The relation gain, bandwidth and noise figure vs bias voltage.

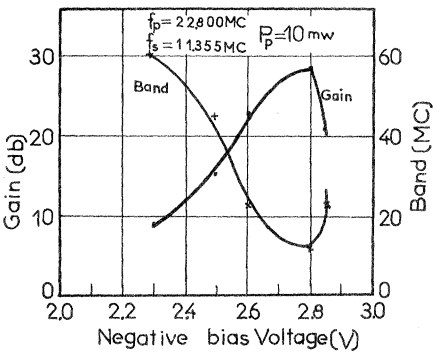

Fig. 5—The relation gain and bandwidth vs bias voltage.

The authors wish to express their gratitude to Dr. T. Fukami, T. Masuda and Dr. B. Oguchi for their interest and encouragement in the work.

S. KITA
F. OBATA
Electrical Communication Lab.
Nippon Telegraph and
Telephone Public Corp.
Tokyo, Japan

Fourier Series Derivation*

Because the Fourier series is never *derived* (it is merely stated and sometimes proved), the following development by Laplace transform should be of interest. The transform of a periodic function $p(t)$ is well known to be

$$P(s) = (1 - \epsilon^{-Ts})^{-1} \int_0^T p(t)\epsilon^{-st}dt, \quad (1)$$

where T=the period. Since $P(s)$ has the set of simple poles $s_n = j2\pi n/T$, $n=0, \pm 1, \pm 2, \cdots$, it has[1] the partial fraction expansion

$$P(s) = \sum_{-\infty}^{\infty} c_n/(s - s_n) \quad (2)$$

where

$$c_n = \lim_{s \to s_n} (s - s_n)P(s)$$
$$= T^{-1} \int_0^T p(t)\epsilon^{-j2\pi nt/T}dt.$$

Hence we obtain the standard exponential form of the series

$$p(t) = \sum_{-\infty}^{\infty} c_n \epsilon^{j2\pi nt/T} \quad (3)$$

by inverting the expansion.

CHRISTOPHER P. GADSDEN
Dept. of Elec. Eng.
Tulane University
New Orleans, La.

Characteristic Impedance of a Slab Line*

A slab line in the form of a central cylindrical conductor between parallel planes is widely used as the slotted section in microwave measurement. Other applications of such a line are found in fields like the dee-stem transmission line inside the dee-chamber of a cyclotron. In these cases, the diameter of the central conductor may be a considerable fraction of the spacing between parallel planes. As such, a comparatively more general expression for the characteristic impedance of such a line is needed. Wholey and Eldred[1] using the transformation $w = \tan z$ derived an expression for the same. However, the expression turns out to be a complex one. A simpler yet reasonably accurate formula is, therefore, desirable. This is obtained in the following manner.

In the case of a central conductor of radius r and the spacing between parallel planes $2s$ we use the transformation $z_1 = \tan \pi z/4s$. This transforms the parallel planes in the z plane to a circle of unit radius in the z_1 plane and the circle of radius r in the z plane to an elliptical shape of semimajor axis $\tan \pi r/4s$ and semiminor axis $\tanh \pi r/4s$ in the z_1 plane. Both these axes are increasing functions of r, and consequently the eccentricity of the transformed ellipse increases comparatively much more slowly with r. This gives the clue that the results obtained for a coaxial transmission line with an elliptical inner conductor[2] may be used without much error up to a value of the diameter-to-spacing ratio as high as 0.75.

Using the transformation

$$\omega = A \ln \left(\frac{z}{k} + \sqrt{\left(\frac{z}{k}\right)^2 - 1} \right),$$

* Received by the IRE, December 17, 1959; revised manuscript received, February 5, 1960.

[1] A theorem justifying this type of expansion is proved in E. T. Copson, "Theory of Functions of a Complex Variable," Oxford University Press, pp. 144–145; 1935.

* Received by the IRE, January 19, 1960.

[1] W. B. Wholey and W. N. Eldred, "A new type of slotted line section," PROC. IRE, vol. 38, pp. 244–248; March, 1950.

[2] S. Mahapatra, "Coaxial transmission lines—effect of elliptical inner conductor on high frequency characteristics," *Elec. and Radio Engr.*, vol. 35, pp. 63–67; February, 1958.

the characteristic impedance of a coaxial transmission line with an elliptical inner conductor of semimajor axis a and semiminor axis b and an outer conductor of radius r is found[2] to be given by

$$Z_0 = 138 \log_{10} \frac{r + \sqrt{r^2 - (a^2 - b^2)}}{a + b} \text{ ohms.}$$

Hence in the case of a slab line with central cylindrical conductor of radius r between parallel planes of spacing $2s$, we get the characteristic impedance as

$$Z_0 = 138 \log_{10} \cdot \frac{1 + \sqrt{1 - (\tan^2 \alpha - \tanh^2 \alpha)}}{\tan \alpha + \tanh \alpha} \text{ ohms,}$$

where

$$\alpha = \frac{\pi r}{4s}.$$

A plot of characteristic impedance Z_0 vs diameter-to-spacing ratio (*i.e.*, r/s) is shown in Fig. 1. It may be noted that this concise formula gives reasonably better approximation up to a value of diameter-to-spacing ratio as high as 0.75. Thus for the values of r/s equal to 0.75, 0.7 and 0.6, the error is found to be about 5, 2.5 and 1 per cent, respectively, and for r/s less than 0.6, the error is negligible. However, the error will sharply increase for values of r/s greater than 0.75.

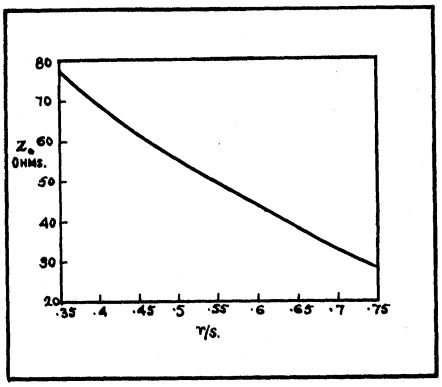

Fig. 1—Characteristic impedance vs diameter-to-spacing ratio.

We note that for values of r/s less than 0.35, we may use, without any appreciable error, the reduced formula,

$$Z_0 = 138 \log_{10} \frac{4s}{\pi r}$$

obtained by Frankel.[3] Knowing the characteristic impedance, we may calculate other parameters of the line.[2]

S. Mahapatra
Elec. Engrg. Dept.
Indian Inst. of Tech.
Powai, Bombay, India

[3] S. Frankel, "Characteristic impedance of parallel wires in rectangular troughs," Proc. IRE, vol. 30, pp. 182–190; April, 1942.

Generating Functions and the Summation of Infinite Series*

A problem often encountered in solving eigenvalue problems is to sum an infinite series of the form

$$\sum_{n=0}^{\infty} a_n \cdot b_n \cdots g_n \cdots \qquad n = 0, 1, 2. \quad (1)$$

An expedient method for manipulating or summing such series is provided by generating functions. Given the generating function

$$G(y) = \sum_{n=0}^{\infty} g_n y^n, \quad (2)$$

then $G(1)$ is the sum of the g_n series, whenever the g_n series converges.

Given the known generating function (2), one can obtain the generating function

$$F(y) = \sum_{n=0}^{\infty} f_n g_n y^n \quad (3)$$

if f_n is a rational polynomial in n. The poles of f_n must be rational or zero. The composition (3) is initiated through the partial fraction expansion of f_n; hence

$$F(y) = \sum_{n=0}^{\infty} \frac{a_0 n^r + a_1 n^{r-1} + \cdots + a_r}{b_0 n^q + b_1 n^{q-1} + \cdots + b_q} g_n y^n$$

$$F(y) = A_m \sum_{n=0}^{\infty} n^m g_n y^n + \cdots + A_0 \sum_{n=0}^{\infty} g_n y^n + \cdots + B_{k-1} \sum_{n=0}^{\infty} \frac{n^{k-1}}{(n+p)^k} g_n y^n + \cdots + B_0 \sum_{n=0}^{\infty} \frac{1}{(n+p)} g_n y^n \quad (4)$$

where p designates the poles; a, b, A and B have positive or negative values and are rational or zero; and k, m, q, and r are integers. The composition is completed by modification of the exponent of the y^n term in (2) so that differentiation or integration with respect to y will yield the desired partial fraction terms of (4).

Let

$$D[G(y)] = \frac{d}{dy} G(y),$$

$$D^{-1}[G(y)] = \int G(y) dy;$$

then, for example,

$$\sum_{n=0}^{\infty} n g_n y^n = yD[G(y)] - C(y^{-s}),$$

$$\sum_{n=0}^{\infty} n^2 g_n y^n = yDyD[G(y)] - C(y^{-s}),$$

$$\sum_{n=0}^{\infty} \frac{g_n y^n}{(n - 1/2)} = y^{1/2} D[y^{-3/2} G(y)] - C(y^{-s}),$$

$$\sum_{n=0}^{\infty} \frac{n}{(n+1)^2} g_n y^n = y^{-1} D^{-1} y^{-1} D^{-1} y^2 D[G(y)] - C(y^{-s}).$$

The $C(y^{-s})$ terms, where $s \geq 0$ and an integer, must be provided in some instances to correct for terms introduced by the operations on $G(y)$ that are not contained in the series expansion of the desired generating function. The number of correction terms cannot exceed the number of operations on $G(y)$. The expression $F(y)$ can then be acquired by summation of the generating functions derived for the expanded terms of (4).

Given (3), a generating function

$$H(y) = \sum_{n=0}^{\infty} f_n g_n h_n y^n \quad (5)$$

can be obtained (f_n need not be present) if h_n is of the form $(u)^n$, where u is any general function but not a function of n. It is evident that

$$H(y) = G(uy) = \sum_{n=0}^{\infty} g_n (uy)^n. \quad (6)$$

A good example of (6) is provided by

$$\sum_{n=0}^{\infty} (i)^n \cos\left[\frac{\pi}{2} n\right] g_n y^n = \tfrac{1}{2}[F(-y) + F(y)].$$

The two procedures just outlined appear rather limited in scope, but can be used to great utility if one expands the factors of (1) into their respective Taylor series. This technique can be demonstrated in the summation of a series of spherical Bessel functions $j_n(x)$ which have the following expansion:

$$\sum_{n=0}^{\infty} j_n(x) = \sum_{n=0}^{\infty} \cdot \left[\sum_{k=0}^{\infty} (-1)^{(n+k)} \frac{2^n k! x^{(2k-n)}}{(2k+1)!(k-n)!}\right]. \quad (7)$$

For large values of the argument x the series (7) is very slowly convergent.[1] The Taylor series expansion of the $j_n(x)$ terms now has made it possible to sum (7) over n to obtain

$$\sum_{n=0}^{\infty} j_n(x) = \sum_{k=0}^{\infty} \frac{x^k}{(2k+1)k!} \left(\sin \frac{\pi}{2} k + \cos \frac{\pi}{2} k\right)$$

which is a form from which the generating function can be found using the procedures of this correspondence. Since

$$y^{-1/2} D^{-1}[\tfrac{1}{2} y^{-1/2}(e^{xy})] = \sum_{k=0}^{\infty} \frac{x^k}{(2k+1)k!} y^k,$$

(7) has the generating function

$$y^{-1/2} D^{-1}[y^{-1/2}(\sin xy - \cos xy)]$$

which upon integration yields for $y = 1$

$$\sum_{n=0}^{\infty} j_n(x) = \frac{\sin x - \cos x}{2x} \cdot \left[1 + 2 \sum_{m=1}^{\infty} \frac{(2m-1)!}{(2m-2)!} (2x)^{-m} \cdot \left(\sin \frac{\pi}{2} m + \cos \frac{\pi}{2} m\right)\right]. \quad (8)$$

When (7) is slowly convergent the right side of (8) is rapidly convergent and vice versa.

The procedures described in this correspondence are certainly not new, but when employed in a systematic manner they can be used to reduce complex series of which the following is an example:

$$ix(\sin\theta) e^{ix \cos\theta} = \sum_{n=0}^{\infty} (i)^n \left[\frac{2n+1}{n(n+1)}\right] P_n'(\cos\theta) j_n(x) \quad (9)$$

[1] H. Feshbach and P. Morse, "Methods of Theoretical Physics," McGraw-Hill Book Co., Inc., New York, N. Y., pp. 1465–1468; 1953.

* Received by the IRE, February 12, 1960.

involving the spherical Bessel function and the associated Legendre polynomial P_n' (cos θ). Relationships such as (9) are often encountered when one seeks solutions to the wave equation in spherical coordinates.

T. H. VEA
Advanced Applications Section
Western Development Laboratories
Philco Corporation
Palo Alto, Calif.

Depth of Penetration as a Measure of Reflectivity of Thin Conductive Films*

The depth of penetration is a measure of the rate at which a wave is attenuated as it progresses in a conducting medium. In the case of very thin metallic films (surrounded on both sides by free space), where the thickness is much less than the depth of penetration, it is conceivable that more of the incident energy is transmitted through the film as it is made thinner. Thus it is desirable to determine the actual decrease in reflectivity as the film thickness is decreased. The investigation yields a multiplicative factor which, when applied to the depth of penetration, is a measure of the required thickness of the film for reflection of a normally incident wave.

A wave normally incident on a thin homogeneous conductive film suspended in free space is considered (Fig. 1). The voltage reflection coefficient is

$$\rho = \frac{Z_{in} - Z_0}{Z_{in} + Z_0} \tag{1}$$

where

Z_{in} = input impedance at the point of incidence,
Z_0 = intrinsic impedance of free space.

$$\rho = \frac{Z_{in} - 377}{Z_{in} + 377}. \tag{2}$$

The input impedance is determined by reflecting the termination impedance Z_R a distance equal to the film thickness l. Thus,

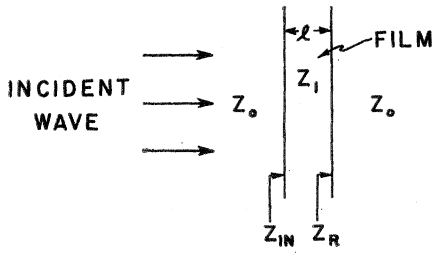

Fig. 1.

* Received by the IRE, February 23, 1960.

$$Z_{in} = \frac{Z_R + Z_1 \tanh \gamma_1 l}{1 + \frac{Z_R}{Z_1} \tanh \gamma_1 l} \tag{3}$$

where

$Z_R = Z_0 = 377$ ohms,
Z_1 = intrinsic impedance of the film,
γ_1 = propagation constant of the film $= \sqrt{j\omega\mu_1\sigma_1}$,
μ_1 = magnetic permittivity of the film (permeability),
ϵ_1 = electric permittivity of the film,
σ_1 = conductivity of the film.

For

$$|\gamma_1| l \leq 0.05,$$

$$Z_{in} = \frac{Z_R + Z_1 \gamma_1 l}{1 + \frac{Z_R}{Z_1} \gamma_1 l}.$$

Since Z_1 is always much less than Z_R for good conductors,

$$\left(\frac{\sigma_1}{\omega\epsilon_1} \gg 1\right);$$

however,

$$Z_{in} = \frac{Z_R}{1 + \frac{Z_R}{|Z_1|} |\gamma_1| l}. \tag{4}$$

Therefore, Z_{in} and ρ are always real.

A reflection coefficient of $\rho = -0.90$ is arbitrarily chosen as the lim ting value for reflection; *i.e.*, to satisfy the condition for reflection it is required that the reflectivity be greater than 90 per cent. Hence, the thickness corresponding to a reflectivity of 90 per cent is referred to as the minimum required thickness for reflection. From (2),

$$\rho' = -0.90 = \frac{Z_{in} - 377}{Z_{in} + 377}.$$

Therefore,

$$Z_{in} = 19.85\ \Omega.$$

Substituting the above value into (4),

$$19.85 = \frac{377}{1 + \frac{377}{|Z_1|} |\gamma_1| l'},$$

$$|\gamma_1| l' = 0.0478\ |Z_1|.$$

Note that, since $|\gamma_1| l$ must be less than, or equal to, 0.05 for $\tanh \gamma_1 l = \gamma_1 l$, $|Z_1|$ must be less than, or approximately equal to, unity.

$$l' = \frac{0.0478\ |Z_1|}{|\gamma_1|}. \tag{5}$$

Also,

$$|\gamma_1| = |\alpha_1 + j\beta_1| = \sqrt{2}\alpha_1 = \frac{\sqrt{2}}{\delta} \tag{6}$$

where

δ = depth of penetration of the film.

Substituting (6) into (5),

$$l' = 0.0338\ |Z_1|\ \delta. \tag{7}$$

Eq. (7) gives the required thickness of the film as a fraction of the depth of penetration for a reflectivity of -0.90. Thus, any thickness greater than l' yields a reflectivity of greater than 90 per cent. With an intrinsic impedance of unity, the minimum required thickness for 90 per cent reflection is only 3.38 per cent of the depth of penetration. Therefore, very thin conductive films with thicknesses in the order of a fraction of the depth of penetration may possess excellent reflective qualities.

Fig. 2 illustrates the manner in which the minimum required thickness l' (in terms of percentage of δ) varies linearly with the intrinsic impedance $|Z_1|$ of the film.

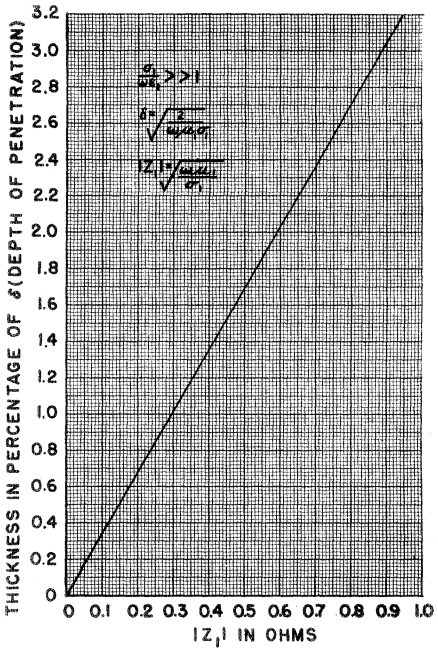

Fig. 2—Variation of minimum required thickness or conductive film with intrinsic impedance for 90 per cent reflectivity.

The actual required thickness for a reflectivity of 90 per cent is

$$l' = \frac{0.0478}{\sigma_1}. \tag{8}$$

Note that (8) is independent of frequency. Thus, the actual minimum required thickness is independent of the depth of penetration to the extent that the depth of penetration is a function of frequency; *i.e.*, for a specific material, the depth of penetration varies with the frequency, whereas the actual minimum required thickness remains constant. For this reason the depth of penetration alone cannot be used as a measure of the reflective properties of a thin conductive film.

It is important to remember that the entire analysis is valid only for good conductors with intrinsic impedances of unity or less.

$$\frac{\sigma_1}{\omega\epsilon_1} \gg 1. \tag{9}$$

$$|Z_1| \leqq 1. \tag{10}$$

The variation of reflection coefficient with film thickness for aluminum at 900 mc is illustrated in Fig. 3. Note that even with a thickness of only 20 Å, the reflectivity is greater than 80 per cent. The conductivity is assumed to be constant at 1.1×10^7 mhos/m. Similar curves may be drawn for frequencies other than 900 mc. For frequencies greater or less than 900 mc, the curves should lie below and above the 900-mc curve, respectively. The lower abscissa, however, is valid only for 900 mc.

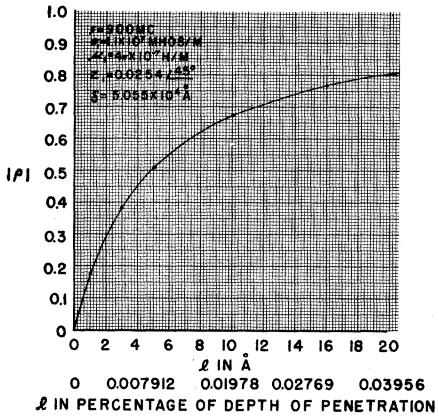

Fig. 3—Reflectivity vs film thickness for aluminum.

Extension of the curve in Fig. 3 to a thickness of 350 Å yields a reflectivity of 98.8 per cent. With this thickness and a frequency of 2000 mc instead of 900 mc, the film still exhibits excellent conductive properties with an intrinsic impedance of less than 0.04 Ω. Thus, according to (8), the coefficient of reflection is still equal to that obtained at 900 mc. For a reflectivity of 98.8 per cent, however, the constant coefficient in (8) and the condition of (10) are different. At all frequencies below 900 mc, the film appears to be, to a greater extent, an excellent conductor, whose intrinsic impedance decreases with decreasing frequency. Thus, the film has a reflectivity of 98.8 per cent for all frequencies below 900 mc. In the case of a sphere with such an aluminum film, then, the lower frequency limit is dependent on the diameter of the sphere.

In all cases satisfying (9) and (10) it is concluded that the minimum required thickness for reflection is a maximum of only 3.38 per cent of the depth of penetration, the percentage decreasing linearly as the intrinsic impedance of the film decreases. The multiplicative factor to be applied to the depth of penetration to obtain the minimum required thickness for a reflectivity of 90 per cent is $0.0338\,|Z_1|$.

F. T. Koide
Collins Radio Co.
Cedar Rapids, Iowa

The Optimum Detection of Analog-Type Digital Data*

An ever-increasing number of communication systems are concerned with the transmission of data. Conventionally, the criterion of good transmission is taken as the ability of the receiver to reproduce the transmitted data as faithfully as possible *i.e.*, that errors be held to a minimum. However, the data transmitted over the communication channel are seldom in their original form. The data may, for example, be the binary representations of an alphabet of numbers which are a code for the English alphabet, as in teletype. On the other hand, the data may be the binary representations of an alphabet of numbers which are a code for the quantized amplitudes of an analog quantity, as in PCM or telemetry.

It is apparent that the effects of errors are different in the two cases cited. The data stream for teletype can be termed "discrete-type" digital data to emphasize that the ultimate output must be discrete; specifically, a letter of the English alphabet must be selected. If the selection is made incorrectly, it is significant only that an error is committed—not what the erroneous selection is. In such a case, minimizing the probability of error is obviously the desirable criterion.

If the receiver output is to be a reproduction of an analog quantity, however, the fidelity with which it can be reconstructed from the imperfectly received stream of "analog-type" digital data becomes the important consideration. Errors committed at the detector are not of interest in themselves, but by virtue of the error magnitudes they reflect into the output.

Minimization of the mean-square error between the original and reconstructed signals is a reasonable criterion to apply to the reception of analog signals. It has the desirable property of penalizing large errors and also has the undeniable advantage of being mathematically tractable in many cases. Applied to speech, it seems a natural criterion since the net effect of reconstruction errors closely resembles that of noise which is usually measured by its mean-square value.

Previous work by the author[1] led to an energy redistribution for the pulses within a PCM code group (to be applied at the transmitter) which minimizes the mean-square error in the receiver output. This reduces the error probabilities for those pulses which contribute heavily to the output at the expense of the less important pulses which add fine detail. Though the error rate at the detector is thereby increased, the output is nevertheless a more faithful reproduction of the original signal.

The mean-square-error criterion can also be used to optimize receiver design by yielding new detector characteristics. The conventional detector for data reception is a decision device yielding one of two distinct outputs at specified intervals. If the final output is to be a sample of an analog signal, then each group of several pulses at the detector will denote (by their polarity, presence-or-absence, etc.) the appropriate coefficients to apply to the binary representation of a particular sample value. Thus, a group of k pulses yields coefficients α_n to permit evaluating the series

$$A = \sum_{n=1}^{k} \alpha_n 2^{n-1}, \qquad \alpha_n = \{0, 1\} \tag{1}$$

where A is the desired sample value.

Consider a binary symmetric channel in which pulses of amplitude $\pm a$ occur periodically in the presence of additive Gaussian noise having unity variance. The conventional detector samples the pulse stream at the appropriate times and makes its decision as to whether the α_n in (1) is a 0 or a 1 according to whether the sample value is negative or positive, respectively. However, the sample value is not intrinsically a discrete quantity. After reconstruction, it will be filtered together with the adjacent sample values to yield a smooth, continuous function of time. Therefore, it is not necessary that α_n be an integer. It is shown in the following that there is a detector characteristic which will yield values for α_n selected from the continuum such that the mean-square error is minimized (though the resulting improvement is rather modest).

The probability densities for the binary symmetric channel are illustrated in Fig. 1.

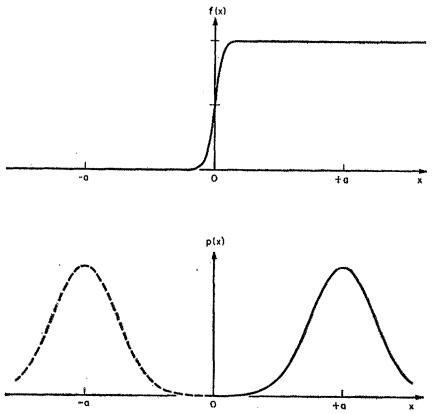

Fig. 1—Probability densities and detector characteristic for the binary symmetric channel, ($a=4$).

Let

$$p(x) = \frac{1}{\sqrt{2\pi}} e^{-x^2/2} \tag{2}$$

denote the density function for the noise. If the transmitted pulse is "positive," its density function is $p(x-a)$ when received in the presence of additive Gaussian noise at a signal-to-noise ratio a^2. Similarly, a "negative" pulse yields a density function $p(x+a)$.

Let $f(x)$ denote the desired detector characteristic. If a positive pulse is to signify the coefficient 1, then receiving it at an amplitude in the interval $(x,\ x+dx)$ causes an error $1-f(x)$ with probability $p(x-a)dx$. A negative pulse, signifying the coefficient 0,

* Received by the IRE, February 15, 1960.

[1] E. Bedrosian, "Weighted PCM," IRE Trans. on Information Theory, vol. IT-4, pp. 45–49; March, 1958.

causes an error $f(x)$ with probability $p(x+a)dx$. For the symmetric channel these events occur with equal probability so the mean-square error can be written

$$\overline{e^2} = \frac{1}{2}\int_{-\infty}^{\infty}[1-f(x)]^2 p(x-a)dx + \frac{1}{2}\int_{-\infty}^{\infty} f^2(x)p(x+a)dx. \quad (3)$$

Minimizing with respect to $f(x)$ is accomplished by setting

$$\frac{\partial \overline{e^2}}{\partial f} = -[1-f(x)]p(x-a) + f(x)p(x+a) = 0,$$

so that

$$f(x) = \frac{p(x-a)}{p(x-a)+p(x+a)} = \frac{1}{1-e^{-2ax}} = \frac{1}{2}+\frac{1}{2}\tanh ax \quad (4)$$

which is plotted in Fig. 1 for $a=4$. It is seen to be symmetrical about $f(0)=\frac{1}{2}$ and to tend monotonically to the exact coefficients, 0 and 1, as asymptotes. For large values of a, *i.e.*, high signal-to-noise ratios, it approaches the characteristic of the conventional detector.

The mean-square error can be evaluated by substituting (4) in (3), giving

$$\overline{e^2} = \frac{1}{2}\int_{-\infty}^{\infty}\frac{p(x+a)p(x-a)}{p(x+a)+p(x-a)}dx = \frac{1}{4}\frac{e^{-a^2/2}}{\sqrt{2\pi}}\int_{-\infty}^{\infty} e^{-x^2/2}\operatorname{sech} axdx. \quad (5)$$

Expanding the exponential in a Maclaurin's series and noting that[2]

$$\int_0^{\infty}\frac{x^{2n}}{\cosh ax}dx = E_n\left(\frac{\pi}{2a}\right)^{2n+1}, \quad a>0,\ n=0,1,2,\cdots, \quad (6)$$

where E_n is the Euler number: $E_0=E_1=1$, $E_2=5$, $E_3=61$, $\cdots$, yields

$$\overline{e^2} \approx \frac{\pi}{4}\frac{e^{-a^2/2}}{\sqrt{2\pi a}}\left[1-\frac{\pi^2}{8a^2}+\cdots\right]. \quad (7)$$

For the conventional detector,

$$f(x) = \begin{cases} 0, & x<0, \\ 1, & x>0, \end{cases} \quad (8)$$

so the mean-square error of (3) becomes

$$\overline{e^2} = \frac{1}{2}\int_{-\infty}^{0}p(x-a)dx + \frac{1}{2}\int_0^{\infty}p(x+a)dx = \int_a^{\infty}p(x)dx \approx \frac{e^{-a^2/2}}{\sqrt{2\pi a}}\left[1-\frac{1}{a^2}+\cdots\right]. \quad (9)$$

Comparing (7) and (9) indicates that the optimum detector decreases the mean-square error in the reconstructed output by a factor of almost exactly $\pi/4$ (about 1 db) for all practical values of a. Of course, an improvement of this magnitude is not of much practical significance since the system with a conventional detector can achieve the same improvement by increasing the pulse amplitude by a factor of 1.025 (for $a=3$) which requires an increase of only 0.2 db in transmitted power. Nevertheless, it is interesting to observe that an improvement is possible and that the optimum detector characteristic resembles the sort of "nonideal" detector characteristic invariably obtained when practical diodes are used.

EDWARD BEDROSIAN
The RAND Corporation
Santa Monica, Calif.

[2] W. Grobner and N. Hofreiter, "Integral Tafel, Zweiter Teil, Bestimmte Integrale," Springer-Verlag, Vienna, Austria, No. 352.1a, p. 163; 1950.

On Network Synthesis with Negative Resistance*

Since the advent of the Esaki diode, there has been an increasing interest in the inclusion of the negative resistance as a basic building block in network theory. The inclusion of this element gives rise to a more general class of function that may be realized as driving point and transfer-impedances. A synthesis procedure will be outlined that enables the synthesis of arbitrary real coefficient, rational functions as driving point or transfer impedances utilizing the following elements: positive resistors, inductors, capacitors, and two-negative resistors. The procedure, in each case, results in networks that are realizable with lossy elements arranged in Foster forms.

Driving Point Impedance Synthesis

Any $Z(s)$ of the form,

$$Z(s) = \frac{N(s)}{D(s)} \quad (1)$$

where N and D are polynomials of arbitrary degree with real coefficients, may be written as

$$Z(s) = Q(s)\frac{\left[\frac{N(s)}{Q(s)}\right]}{D(s)} \quad (2)$$

where

$$Q(s) = \prod_{i=1}^{n}(s+a_i);\ a_i \text{ real}, \quad 0<a_1<a_2<a_3\cdots,$$

and n is one greater than the degree of N or D, whichever is larger.

Utilizing the technique demonstrated by Kinariwala,[1] (2) may be expanded as

$$Z(s) = \frac{Q}{D}\left[\frac{N_1}{D_1}-\frac{N_2}{D_2}\right] = \frac{D_2N_1}{D} - \frac{D_1N_2}{D}, \quad (3)$$

where

$$\frac{N_1}{D_1} \text{ and } \frac{N_2}{D_2}$$

are both RC r.p. functions. Since $Q=D_1D_2$, D_2N_1 and D_1N_2 are strict RC Hurwitz Polynomials[2] of degree $n-1$. Now defining

$$Z(s) = \frac{1}{Y_1}+\frac{1}{Y_2}, \quad (4)$$

we can identify

$$Y_1 = \frac{D}{D_2N_1}, \quad (5)$$

and

$$Y_2 = \frac{-D}{D_1N_2}. \quad (6)$$

The degrees of the denominators of Y_1 and Y_2 (which are strict RC Hurwitz polynomials) are equal to or greater than D. A simple extension of the above technique will enable the final synthesis.

Theorem: Any rational function $Y(s)$, whose denominator is a strict RC Hurwitz polynomial and of degree greater than or equal to the numerator, may be expanded into the sum of an RL Foster form, an RC Foster form, and one negative constant.

Proof:

$$Y(s) = \frac{N}{\prod_{y=1}^{m}(s+b_y)} = \sum_{k=1}^{m_1}\frac{|d_k|}{s+b_k} - \sum_{i=1}^{m_2}\frac{|e_i|}{s+b_i} = \sum_{k=1}^{m_1}\frac{|d_k|}{s+b_k} + \sum_{i=1}^{m_2}\frac{s\left|\frac{e_i}{b_i}\right|}{s+b_i} - \sum_{i=1}^{m_2}\left|\frac{e_i}{b_i}\right|$$

where

$$m_1+m_2=m.$$

Thus

$$Y(s) = Y_1(s)+Y_2(s)-R,$$

where

$$Y_1(s) = \sum_{k=1}^{m_1}\frac{|d_k|}{s+b_k} \quad \text{(an RL foster form)},$$

and

$$Y_2(s) = \sum_{i=1}^{m_2}\frac{s\left|\frac{e_i}{b_i}\right|}{s+b_i} \quad \text{(an RC Foster form)},$$

$$-R = \sum_{i=1}^{m_2}\left|\frac{e_i}{b_i}\right| \quad \text{(one negative resistor)}.$$

Therefore, (5) and (6) may be expanded as:

$$Y_1 = Y_3+Y_4-R_1 \quad (7)$$

$$Y_2 = Y_5+Y_6-R_2, \quad (8)$$

where Y_3 and Y_5 are RL Foster forms, and Y_4 and Y_6 are RC Foster forms. The network corresponding to (4), (7), and (8) is shown in Fig. 1.

Note that since the number of reactive elements or positive resistors in both the Y_1 and Y_2 realizations is equal to the degree of N or D (whichever is greater), the total quantity of each is at most twice this number.

Transfer Impedance Synthesis

The network shown in Fig. 2 yields an open-circuit voltage ratio which may be ex-

* Received by the IRE, March 24, 1960.

[1] B. K. Kinariwala, "Synthesis of active RC networks," *Bell Sys. Tech. J.*, vol. 38, p. 1302; September, 1959.

[2] Polynomials with simple negative real roots none of which are zero.

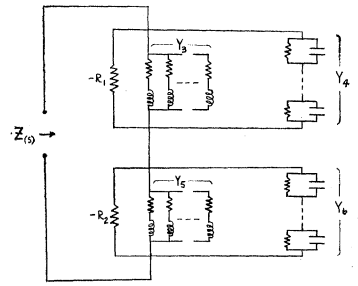

Fig. 1.

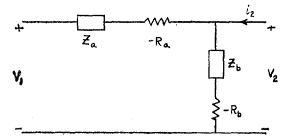

Fig. 2.

pressed as

$$\left.\frac{v_2(s)}{v_1(s)}\right|_{i_2=0} = \frac{Z_b - R_b}{Z_b - R_b + Z_a - R_a} = \frac{1}{1 + \dfrac{Z_a - R_a}{Z_b - R_b}}. \quad (9)$$

The prescribed transfer impedance, however, may be written as

$$\left.\frac{v_2(s)}{v_1(s)}\right|_{i_2=0} = \frac{N(s)}{D(s)} = \left[\frac{1}{1 + \dfrac{D-N}{N}}\right] \quad (10)$$

where N and D are polynomials of any degree with real coefficients. From (9) and (10) the following identification is made

$$\frac{Z_a - R_a}{Z_b - R_b} = \frac{D-N}{N}, \quad (11)$$

which may also be expressed as

$$\frac{Z_a - R_a}{Z_b - R_b} = \frac{\dfrac{D-N}{Q}}{\dfrac{N}{Q}}, \quad (12)$$

with

$$Q(s) = \prod_{i=1}^{m} (s + a_i)^3$$

where m is equal to the degree of D or N, whichever is larger. Utilizing the previous theorem the right side of (12) can be expanded as

$$\frac{\dfrac{D-N}{Q}}{\dfrac{N}{Q}} = \frac{Z_1 + Z_2 - R_1}{Z_3 + Z_4 - R_2}, \quad (13)$$

where Z_1 and Z_3 are RL Foster forms, Z_2 and Z_4 RC Foster forms. Thus according to (12), we may make the identification

$$\begin{aligned} Z_a &= Z_1 + Z_2 \\ Z_b &= Z_3 + Z_4 \\ -R_a &= -R_1 \\ -R_b &= -R_2, \end{aligned}$$

[3] Where $Q(s)$ is subject to the same restrictions as in the previous case.

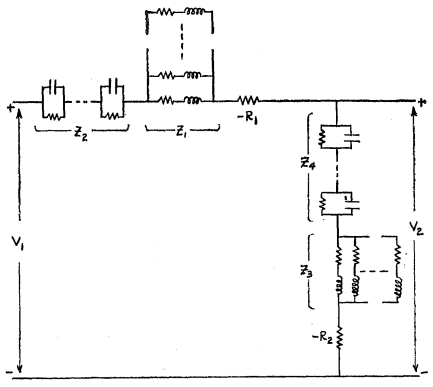

Fig. 3.

and the network of Fig. 2 becomes that shown in Fig. 3.

Note that the total number of reactive elements or positive resistors is equal to or less than twice the degree of N or D, whichever is larger.

It is anticipated that a more complete paper will be submitted at a later date.

F. T. Boesch
M. R. Wohlers
Dept. of Elec. Engrg.
Polytechnic Inst. of Brooklyn
Brooklyn 1, N. Y.

Electromagnetic Energy in a Dispersive Medium*

The energy density of the electromagnetic field in a dispersive medium was recently discussed by Hosono and Ohira.[1] It should be noted that their results had already been given by Levin[2] and derived still earlier by Rytov in references quoted by Levin.

It is of interest that the dispersive forms of the energy are also those required for the mean thermal fluctuation energy of the electric (or magnetic) fields in a CR (or LR) circuit to comply with the equipartition principle. Consider such a circuit, in which R is made very large compared with loss resistance of the capacitor (or inductor), which inevitably occurs when the permittivity (or permeability) is dispersive by virtue of the Kramers-Kronig relations. Then the mean energy of the electric field in the capacitor is given by

$$\int_0^\infty \frac{4kTR}{1 + (\omega CR)^2} \cdot \frac{1}{2} \frac{d}{d\omega}(\omega C) \cdot df = \frac{1}{2} kT$$

and similarly the mean energy of the magnetic field in the inductor is

$$\int_0^\infty \frac{4kTR}{\omega^2 L^2 + R^2} \cdot \frac{1}{2} \frac{d}{d\omega}(\omega L) \cdot df = \frac{1}{2} kT.$$

It may readily be shown that these results are independent of the geometry of the capacitor or inductor.

R. E. Burgess
Dept. of Physics
University of British Columbia
Vancouver, Canada

* Received by the IRE, March 10, 1960.

[1] T. Hosono and T. Ohira, "The electromagnetic energy stored in a dispersive medium," Proc. IRE, vol. 48, pp. 247–248; February, 1960.

[2] M. L. Levin, "An elementary derivation of the formula for the electromagnetic energy in a dispersive medium," *J. Exper. and Theoret. Phys.*, vol. 29, p. 252; August, 1955. Also in *Soviet Phys. JETP*, vol. 2, pp. 168–169; February, 1956.

Determination of Satellite Orbits from Radar Data*

The present paper is a report on an investigation of methods for the determination of satellite orbits from radar data. Of particular interest are problems which require the rapid calculation of the orbit elements from a limited amount of data. In some cases the available information may be restricted to the data obtained from a single pass, over a period of 2 to 4 minutes, as the satellite goes by the observing station. The solution to this computing problem requires methods which are rather different from those developed previously for the calculation of satellite orbits from observations extending over several revolutions of the satellite.

The following section describes in some detail a method which has been found to offer a good combination of speed and accuracy. It requires between 10 and 20 seconds for a rough determination, yielding orbit elements in this time with a precision of 0.001 in eccentricity and 0.05 minutes in period. This degree of accuracy is sufficient to determine whether the satellite is in orbit. The program then proceeds automatically with a correction routine which operates on the preliminary orbit elements to yield a more accurate prediction of the position of the satellite at later points along the orbit. The precision of the corrected predictions is 500 yards or better, which is sufficient for the purpose of acquisition by other radars at later points along the orbit. This correction routine requires an additional 40 seconds of computer time.

Procedure

The procedure chosen as optimum involves the following steps:

Orbit Inclination

A plane is passed through the center of the earth and through all the points along the radar track. The inclination of the plane and the position of the line of nodes are adjusted to the full set of data by a least-squares calculation. The plane of the orbit is now determined.

Orbit Elements in the Plane

The three orbit elements in the plane must still be determined after the plane of the orbit has been fixed. These may be taken

* Received by the IRE, March 18, 1960.

as the period, perigee altitude, and argument of perigee. They can be computed from any three items of information along the track. We have found it most accurate to choose 2 points on the track and the time between them as our three fundamental items. The procedure for the calculation of the orbit elements depends in an essential way on the dynamics of the satellite motion, and may be called the *dynamical* method. It is also known as the method of Gauss and Olbers.

Full use is made of the data by dividing the track into halves, and pairing the points in the first half with those in the second half in chronological order. The final orbit elements are obtained by taking an average of the individual results. A least-squares method is usually used instead, but we have found that the least-squares procedure does not, in fact, offer any advantage over the method of simple averages. The orbit elements obtained in this way are printed out as immediate results.

Differential Correction of the Orbit Elements

In the third step of the computation the slant ranges are used for a further improvement. The slant ranges are the most accurate elements of the radar data, and it is necessary to devote special attention to them at the end of the computing procedure in order to extract the greatest orbital precision from the tracking data. The adjustment of the orbit elements to the slant ranges is carried out by conventional differential correction routines.

A special procedure is used for orbits of an eccentricity less than 0.01. In this procedure a circular orbit is assumed as the first approximation to the results. The effects of the ellipticity are added as a small correction to the circular orbit. The program for the low-eccentricity calculation is extremely simple and requires an additional computing time of only 5 seconds if the supplementary procedure is incorporated into the main program described above. The accuracy of the supplementary method is the same as that given in the main procedure. In the actual computing operation the results of both procedures can be printed out in parallel, and the appropriate set of answers chosen by inspection of the computed eccentricity, or the choice can be made internally in the program, and a single answer printed out.

Other Possibilities for a Short Program

Other methods for the rapid determination of the orbit elements have been investigated, including: 1) a purely geometrical procedure in which an ellipse is passed through 3 data points along the track, again with the center of the earth as focus; this method does not make use of the dynamical equations of the satellite motion, and was investigated because the basic equations are exceedingly simple; however, it was found to be considerably less acurate than the dynamical or Gauss-Olbers procedure; 2) a least-squares adjustment of the orbit elements in place of the average; the results obtained by the least-squares method are inferior to the direct average in accuracy for short arcs (less than 4 minutes).

Table I presents a comparison of the results obtained from these methods.

TABLE I
Errors in Orbit Elements for Equally Spaced Points Along an Arc

	Gauss-Olbers (4-minute arc)	Geometric (4-minute arc)	Least-Squares Geometric ($6\frac{1}{2}$-minute arc)
Period (minutes)	0.004	0.06	0.09
Argument Perigee (degrees)	0.02	0.3	0.4
Perigree Altitude (miles)	0.3	0.8	2.3

Accuracy

The errors in the computation of the orbit elements are listed below for the typical case of a radar pass lasting two minutes (these results constitute the average over 20 data points, selected in two groups of 10 points each at one second intervals at the beginning and end of the radar track):

0.004	minutes in period.
0.200	miles in perigee height.
0.15	degrees in perigee argument.
0.001	degrees in angle of inclination.

The above errors in orbit elements will produce the following uncertainties in the position of the satellite after $\frac{1}{3}$ of a revolution:

300	yards along the track.
300	yards normal to the track in the orbit plane.
150	yards normal to the orbit plane.

The major portion of the uncertainty in position perpendicular to the track comes from the error in period (from which the mean radius is computed); the error in eccentricity contributes only an uncertainty of 0.04 mile in this direction.

Computing Rime

One minute of IBM 704 time is required for the determination of the orbit elements from one radar pass including 20 data points. By eliminating the differential correction routine, the computing time can be reduced to between 10 and 20 seconds, at the sacrifice of a factor of 10 in the accuracy of the orbit determination. In this latter case, the errors are approximately 5 miles in positional uncertainty, or 0.001 in eccentricity and 0.05 minutes in period. These errors are too great for the abbreviated determination to be useful in the acquisition of the orbit by other radars, but they are adequate to provide a decision as to whether the satellite is in orbit.

I. Harris
W. F. Cahill
Theoretical Div.
Goddard Space Flight Center
NASA
Washington, D. C.

A Traveling Wave Harmonic Generator*

In conventional harmonic generators the supply of harmonic power to the load is periodic at the fundamental frequency. This means that, as well as the wanted harmonic, unwanted harmonics are also generated. If the supply of power to the load could be arranged to be periodic at the harmonic frequency then this disadvantage could be overcome. Fig. 1 shows a device in which this is achieved. Power at the fundamental frequency F is fed to the input of a propagating structure that has n diodes connected to it as shown. Arrangements to supply dc bias to the diodes must be included. As the fundamental wave travels down the structure the diodes conduct in turn and pass pulses to the load R_L. If the delay per section is chosen to be $\{1/nF\}$ seconds and the bias adjusted so that only one diode is conducting at any time then the principal component of the voltage across R_L will be at a frequency of nF.

In traveling down the line the fundamental wave will be attenuated due to dissipation in the line and power fed to R_L. This can be compensated to a certain extent by progressively reducing the dc bias on the diodes.

If the device is made using distributed elements then it may not be convenient to connect all the diodes together to one point. In this case the diodes may be connected to a second propagating structure at distances equal to an integral number of wavelengths at the harmonic frequency.

If a circulator is available then the power that would otherwise be last in R_T can be conserved by connecting the output of the line back into the circulator as shown in Fig. 2.

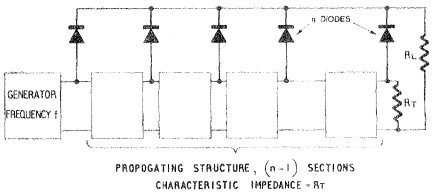

Fig. 1.

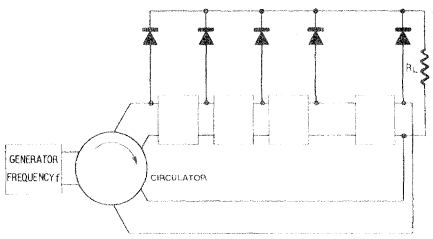

Fig. 2.

D. L. Hedderly
British Telecommunications Res., Ltd.
Taplow Court, Berks., Eng.

* Received by the IRE, March 29, 1960.

A Realization Theorem for Biquadratic Minimum Driving-Point Functions*

Kim[1] has introduced a method of synthesis for biquadratic minimum impedance functions in the form of an unbalanced bridge containing five elements. According to this method the network topology is first assumed, after which the driving-point impedance function is derived in terms of the branch elements and compared to the impedance function to be realized. The method always necessitates the augmentation of the impedance function with surplus factors. In a later publication, Van Valkenburg[2] stated the necessary conditions on the coefficients of biquadratic minimum impedance functions to be realizable in two special bridge forms with only five elements, but no derivation or proof was given. This letter not only presents a useful theorem for the synthesis of biquadratic minimum driving-point functions, but also gives a more general method of synthesis which leads directly to the results given by Kim and Van Valkenburg.

We begin with the positive real biquadratic impedance function

$$Z(s) = K\frac{s^2 + a_1 s + a_0}{s^2 + b_1 s + b_0}. \tag{1}$$

This function will be minimum, that is $Z(j\omega_1) = 0 \pm jX(\omega_1)$ at one ω_1 with $X(\omega_1) \neq 0$, only if

$$(\sqrt{a_0} - \sqrt{b_0})^2 = a_1 b_1. \tag{2}$$

The function (1) can be represented as the driving-point impedance to an RL two-port network terminated in a single capacitance. Such a representation is shown schematically in Fig. 1(a). A driving-point impedance function $Z(s)$ is related to the terminating capacitance and the open-circuit impedance

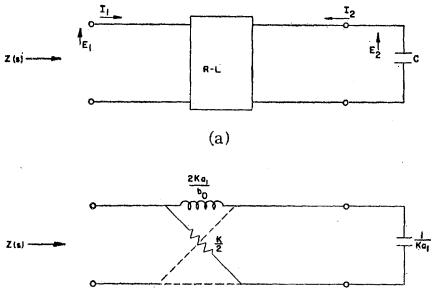

Fig. 1.

parameters of a two-port by the relation

$$Z(s) = z_{11}\frac{1 + sC\dfrac{1}{y_{22}}}{1 + sC(z_{22})}. \tag{3}$$

We now seek to express (1) in the form of (3). This is done by writing the former as

$$Z(s) = K\frac{a_1 s + a_0}{b_0}\,\frac{1 + sc\dfrac{s}{(a_1 s + a_0)C}}{1 + sc\dfrac{s + b_1}{b_0 C}}, \tag{4}$$

from which we make the identifications

$$z_{11} = K\frac{a_1 s + a_0}{b_0}, \qquad z_{22} = \frac{s + b_1}{b_0 C},$$
$$y_{22} = \frac{(a_1 s + a_0)C}{s}. \tag{5}$$

Eqs. (5) define a set of positive real RL driving-point functions. We have still to find a rational function representation of z_{12}. Recall that

$$z_{12}^2 = z_{11}\left(z_{22} - \frac{1}{y_{22}}\right). \tag{6}$$

Hence from (5) and (6) we have

$$z_{12} = \sqrt{\frac{a_1 s^2 + (a_1 b_1 + a_0 - b_0)s + a_0 b_1}{b_0^2/CK}}. \tag{7}$$

The quantity under the radical of (7) is always a perfect square, as comparison with (2) verifies, and so the open-circuit transfer impedance function reduces to

$$z_{12} = \frac{S + \dfrac{a_1 b_1 + a_0 - b_0}{2a_1}}{b_0\sqrt{C/a_1 K}}. \tag{8}$$

It can be easily verified that the residue and real-part conditions are always satisfied with the equal sign. Hence the poles are compact. This, plus the positive real character of the two RL driving-point impedances of (5), assures us that z_{11}, z_{22}, and z_{12} represent a physically realizable RL two-port network. This constitutes sufficient proof for establishment of the following theorem.

> Theorem: Any biquadratic minimum driving-point impedance function can be realized as the input to an RL two-port network terminated in a single capacitance.

Although a realization of $Z(s)$ is always possible according to the theorem, it is not impossible to say that no inductive coupling is necessary, or that the realization will yield a minimum number of elements. For obvious reasons, however, we seek those realizations which involve no inductive coupling. This means that the Fialkow-Gerst conditions must be satisfied. For this simple case we find, because of the compact nature of the poles, that this is possible only if the corresponding residues of the poles of z_{11}, z_{22}, z_{12} are equal. This implies that $z_{11} = z_{22}$, and so an additional restriction is imposed on the coefficients of $Z(s)$ in the form

$$\frac{a_0}{b_0} = 1/4. \tag{9}$$

The open-circuit impedance parameters of the two-port finally reduce to

$$z_{11} = z_{22} = K\frac{a_1 s + a_0}{b_0}, \qquad z_{12} = K\frac{a_1 s - a_0}{b_0}, \tag{10}$$

which we recognize to be realizable in the form of a symmetrical lattice containing two reactive and two resistive elements. The network which realizes (1) is shown in Fig. 1(b).

The case treated above suggests the possibility of representing the function $z(s)$ as the input to an RC two-port network terminated in a single inductance. However, since the necessary and sufficient conditions for the realization of the complete impedance matrix as an RC two-port are still unknown, we cannot hope to achieve results as general as before. For this representation, shown schematically in Fig. 2(a), (3) is modified to give

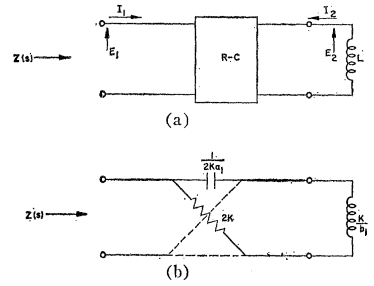

Fig. 2.

$$Z(s) = K\frac{s + a_1}{s}\,\frac{1 + \dfrac{1}{sL}\dfrac{a_0 L}{s + a_1}}{1 + \dfrac{1}{sL}\dfrac{(b_1 s + b_0)L}{s}}, \tag{11}$$

from which we find

$$z_{11} = K\frac{s + a_1}{s}, \qquad z_{22} = \frac{(b_1 s + b_0)L}{s},$$
$$y_{22} = \frac{s + a_1}{a_0 L}. \tag{12}$$

From (2), (6), and (12) we compute the open-circuit transfer function to be

$$z_{12} = \frac{s + \dfrac{b_0 + a_1 b_1 - a_0}{2b_1}}{(1/\sqrt{b_1 KL})S}. \tag{13}$$

Since the coefficients are always positive, the two open-circuit impedances of (12) represent positive real RC driving-point functions. Also, a check of the residue and real-part conditions again shows that they are satisfied with the equality sign. Because of the compact nature of the poles the only way we can possibly obtain a realization of $Z(s)$ as the input to an RC two-port terminated in a single inductor is for the corresponding residues of the poles of z_{11}, z_{22}, and z_{12} to be equal, in which case the Fialkow-Gerst conditions are automatically satisfied. Again $z_{11} = z_{22}$ so that the resulting restriction on the coefficients of $Z(s)$ will be

$$a_0/b_0 = 4. \tag{14}$$

The open-circuit impedances of the two-port now become

$$z_{11} = z_{22} = K\frac{s + a_1}{s}, \qquad z_{12} = K\frac{s - a_1}{s}, \tag{15}$$

which are realizable as a symmetrical lattice. The complete network is shown in Fig. 2(b).

The method of synthesis of biquadratic minimum functions presented here has yielded directly the two networks of Figs. 1(b) and 2(b), both of which contain a mini-

* Received by the IRE, March 7, 1960.

[1] W. H Kim, "A New Method of Driving-Point Function Synthesis," Electrical Engineering Research Lab., Rept. No. 1, Contract DA-11-022-ORD-1983, University of Illinois, Urbana; April 1, 1956.

[2] M. E. Van Valkenburg, "Special case of a bridge equivalent of Brune networks," PROC. IRE, vol. 44, p. 1621; November, 1956.

mum number of elements. No prior assumption was made as to their topological form, nor was any augmentation of the impedance function with surplus factors required as in Kim's method. Furthermore, the nature of the reactance $X(\omega)$ at the frequency ω_1 is of no consequence with the method presented here, and so need not be considered. In addition, (9) and (14), which are a direct consequence of the method of realization, are precisely those conditions on the coefficients of $Z(s)$ stated earlier by Van Valkenburg.

K. B. Irani
C. P. Womack
Dept. of Elect. Engrg.
University of Kansas
Lawrence, Kans.

Transformation of Impedances Having a Negative Real Part and the Stability of Negative Resistance Devices*

I. Transformation of Impedance

If a circuit element possessing a negative real part terminates one end of a transmission line, the magnitude of the reflection coefficient will, in general, be greater than unity. At first glance, it would appear that the standard transmission line calculator (Smith Chart[1]) would have to be expanded beyond $\rho=1$ (ρ is the reflection coefficient) in order that it can be used for finding the values of transformed impedances (admittances). However, as will be shown below, the present Smith Chart can be used if the radius sector is interpreted as the reciprocal of the reflection coefficient.

Basically, as is well known, the Smith Chart is the plot of the real and imaginary parts of the function.

$$\frac{1+\rho e^{2j\theta}}{1-\rho e^{2j\theta}}$$

in the plane where ρ and θ are polar co-ordinates; ρ is the reflection coefficient and θ is the electrical phase angle. A method for transforming impedances with a negative real part can be obtained by use of the following identity:

$$\frac{1+\rho e^{2j\theta}}{1-\rho e^{2j\theta}} = -\frac{1+\frac{1}{\rho}e^{-2j\theta}}{1-\frac{1}{\rho}e^{-2j\theta}} \tag{1}$$

and its equivalent

$$\frac{Z}{Z_0} = -\left\{\frac{-Z_L+jZ_0\tan(-\theta)}{Z_0+j(-Z_L)\tan(-\theta)}\right\} \tag{2}$$

where

Z_0 = characteristic impedance of line
Z_2 = terminating impedance
Z = transformed impedance.

The procedure for transforming the impedance

$$Z_L = -R+jX,$$

through the electrical angle θ along a line of characteristic impedance using the Smith Chart, is as follows:

1) Normalize the impedance and form its negative:
$$+\frac{R}{Z_0}-j\frac{X}{Z_0}.$$
2) Plot this point on the Smith Chart.
3) Use the Smith Chart in the usual fashion except that the angular direction is opposite; *i.e.*, go "toward load" when physically the transformation is "toward generator" and conversely.
4) Take the negative of the reading on the Chart and multiply by Z_0 for the final result.
5) The reflection coefficient is the reciprocal of that given on the Chart.
6) The standing wave ratio is the negative of that on the Chart.
7) Use a similar procedure for transforming admittances.

In the case that the line has a loss per unit length given by the real part of the complex propagation factor γ, where

$$\gamma l = \alpha l + j\beta l \equiv \alpha l + j\theta, \tag{3}$$

we must use a procedure similar to that used for ordinary impedances except to spiral outward instead of inward. This corresponds to replacing

$$\frac{1}{|\rho|} \text{ by } \frac{1}{|\rho|e^{-2\alpha l}} = \frac{e^{2\alpha l}}{|\rho|}.$$

If

$$\alpha l', \qquad 0 \le \beta l' \le \beta l \equiv \theta$$

is such that the rim of the Chart may be reached, we then have a transition from negative to positive input resistance. This, of course, corresponds to the physical situation, in that energy production by the active element is balanced by energy loss in the line.

II. Stability of Negative Resistance Devices

In low frequency series-fed circuits employing devices which possess negative resistance and series reactive elements, the condition for stability against oscillation is that the positive resistance (sink of energy) must exceed the negative resistance (source of energy). If the positive and negative resistances are separated by a finite length of transmission line, this condition is not sufficient, since the positive resistance may only lightly load the negative resistance device.

For the remainder of this section, we shall consider the shunt-fed circuit shown in Fig. 1. It consists of a contact current generator whose equivalent admittance is Y_+, connected to a transmission of characteristic admittance Y_0 and length L. The line is terminated in an admittance Y_- which has a negative real part. The condition for stable oscillations is that

$$Y_+ = -Y_-' \tag{4}$$

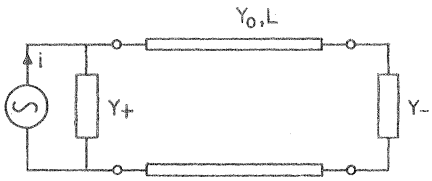

Fig. 1.

where

$$-Y_-' = \frac{(-Y_-)+jY_0\tan(-\theta)}{Y_0+j(-Y_-)\tan(-\theta)};\ \theta=\beta L. \tag{5}$$

Note that the value of Y_-' as a function of frequency (through θ) is given by the locus of points on the Smith Chart corresponding to the transformation given in section I for different values of θ. If the frequency band considered is sufficiently large, the curve will have to be continued on separate sheets). Similarly the values of Y_+/Y_0 as a function of frequency can be plotted on the Chart; a necessary condition for stability is that the two curves do not intersect. However, this condition is not sufficient, for two reasons:

1) It does not rule out the possibility of growing oscillations.
2) Because of nonlinearities, the absolute value of the real part of Y_- may range from zero to a maximum value (for example, a tunnel diode).

We can take the second factor into account by considering the locus to consist of the entire region bounded on the outside by the sum of the Chart ($|\rho|=1$), and on the inside by the locus determined from $|Rl\ Y_-|$ having its maximum value. The sufficient condition for stable amplification is then that the locus Y_+/Y_0 does not enter into this region.

The criterion conforms to the usual criteria for stable operation. First, for vanishingly-small θ it is assumed that:

$$|RlY_+| > |RlY_-| \tag{6}$$

which is the condition for stable operation when the positive and negative conductances are located at points of equivalent electrical phase. Secondly, at any frequency, it implies that

$$|\rho_+| < \frac{1}{|\rho_-|}, \quad |\rho_+\rho_-| < 1$$

(cf. section I, Procedure, step 5) (7)

where $\rho_\pm$ are the reflection coefficients for the line terminated in $Y_\pm$. This condition[2] also insures that the Laplace transform of the current and voltage, at any point on the line, has no poles in the half-plane.

$$Rls = Rl(\sigma+j\omega) \ge 0$$

where s is the complex frequency variable.

Bernard Rosen
RCA
Surface Communication Lab.
75 Varick St.
New York, N. Y.

* Received by the IRE, February 17, 1960.

[1] H. P. Smith, "Transmission line calculator," *Electronics*, pp. 29–31; January, 1939.

[2] E. Weber, "Linear Transient Analysis," John Wiley and Sons, Inc., New York, N. Y., vol. 2, pp. 285–286; 1956.

Relativity: Blessing or Blindfold?*

The latest attempt to measure an ether drift (with the ammonia maser) gave the expected zero drift but with a much improved accuracy.[1] For some time the preferred interpretation of a null ether drift has been confirmation of the special theory of relativity and rejection of an ether. However, a second interpretation, based on the Fitzgerald-Lorentz contraction theory, also explains the null result but allows an ether. The special theory was originally preferred because of the *ad hoc* nature of the Fitzgerald-Lorentz theory. This *ad hoc* stigma has since been removed by Ives' classical derivation of the Lorentz transformations.[2] Furthermore, Ives has extended the Fitzgerald-Lorentz theory to explain the three famous tests of general relativity: the advance of the perihelion of Mercury[3] and the bending and frequency shift of light in a gravitational field.[4] Thus, a theoretical superiority of the relativistic interpretation is now questionable.

There is a major physical difference between the two theories: The special theory requires that the measured one-way velocity of light in a vacuum, c, be constant, while the Fitzgerald-Lorentz theory requires only that the measured average velocity of an out-and-back light signal be constant and equal to c. This difference has not yet been put to a proper test. All experiments to date, including the maser experiment,[1] give the average velocity of a two-way light signal, or the equivalent. A variation in the one-way velocity of light with direction in space (in the absence of a significant gravitational field) is *prima-facie* evidence for the existence of an ether.

Resolution of the ether problem is requisite for our efforts to fathom the hypostasis of matter and radiation. The present abundance of electrical particles has been compared to the enigmatic profusion of chemical elements before the discovery of the electron, and is considered to herald the discovery of a subelectrical form of matter. Is this subelectrical matter the constituent of a ubiquitous ether which forms an invisible sea in which the electrical particles (and radiation) exist; or is this subelectrical matter confined only to the electrical particles (and quanta)? Resolution of the ether question can be of considerable heuristic value here. Continued emphasis on the special theory detracts from the need for a crucial experiment.

Maxwell[5] was the first to propose a one-way measurement from observations of astronomical objects. Much later Bottlinger[6] suggested this as a test of relativity. Courvoisier,[7] following his suggestion, found, from the 1908–26 eclipse observations of Jovian satellites, an ecliptic component of the sun's motion through an ether of 715 ±95 km/sec directed at an angle of 132° ±6°. However, this result is not very convincing because the observed variation, which is somewhat less than the probable error in the eclipse observations, can also result from some flaw in the complicated and incomplete gravitational theory of the Jovian system.

An independent evaluation of the timing error due to the motion of the earth alone should overcome this objection of gravitational theory. In Fig. 1 the heliocentric longitudes of a planet, the earth and the light ray are respectively θ, ϕ, and ψ, with respect to the direction of the First Point of Aries, Υ. It is assumed that the component of the sun's motion through an ether in the ecliptic plane is w at angle α, $w \ll c$, and the paths of the earth and planet are coplanar.

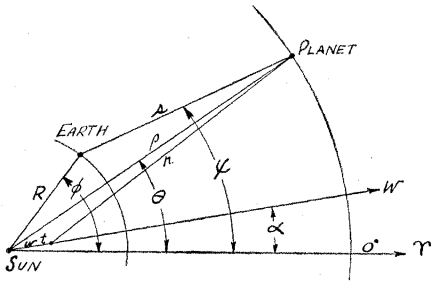

Fig. 1—Relation of sun, earth and planet.

Terms above the first order are neglected. Lorentzian variations in length, time, and mass therefore do not apply. During the time $t=\rho/c$ required for reflected light to return to the sun, the sun moves a distance wt in the ether. For a heliocentric observer, the error in determining the planet's position (calculated minus observed time) is

$$\Delta t_h = \rho/c - r/c = \rho(w/c^2)\cos(\theta-\alpha) \quad (1)$$

since, from the geometry

$$r = [(\rho\cos(\theta-\alpha) - wt)^2 + \rho^2\sin^2(\theta-\alpha)]^{1/2} \cong \rho - \rho(w/c)\cos(\theta-\alpha). \quad (2)$$

Similarly, with respect to a geocentric observer, the earth moves a distance wt in the calculated time s/c, to give a time error of

$$\Delta t_g = \pm s(w/c^2)\cos(\psi-\alpha) \quad (3)$$

where the plus and minus signs apply for outer and inner planets respectively. The two timing errors, (1) and (3), differ because the positions of the earth and sun do not coincide. The difference, which is the timing error due to the path of the earth, is

$$\Delta t_e \equiv \Delta t_g - \Delta t_h = -R(w/c^2)\cos(\phi-\alpha) \quad (4)$$

since $R\cos(\phi-\alpha) \pm s\cos(\psi-\alpha) = \rho\cos(\theta-\alpha)$, where the plus and minus signs apply as above. The result is independent of the observed object provided the object is not an earth satellite.

The timing error Δt_e should exist simultaneously with Δt_h and Δt_g in the residuals from calculated and observed times of astronomical observations. The relative error $\Delta t_e/R$ should then be equal in amplitude and opposite in phase to $\Delta t_h/\rho$ and for outer planets $\Delta t_g/s$. It would be difficult to explain how classical gravitational theory, *without specifying an anisotropy of space*, could introduce into two unrelated motions, such as those of the earth and a planet, a common periodic error referenced to some arbitrary direction in space. Courvoisier approximated the heliocentric error (1), but did not evaluate the independent timing error due to the earth. Analysis of a sufficient number of residuals of past astronomical observations with modern computers should permit an unambiguous check for a variation in the one-way velocity or light.

Because of the paucity of suitable astronomical objects substantially outside the ecliptic plane, past observations can only yield the ecliptic component of the sun's motion through an ether. Hence, experiments with artificial satellites are desirable to explore the direction normal to the ecliptic plane. For an earth satellite, the derivation of the timing error is the same as for (1). This may be rewritten for a satellite as

$$\Delta t_s = S(v/c^2)\cos\gamma \quad (5)$$

where S is the distance between observer and satellite, v is the velocity of the observer through the ether, and γ is the angle between S and v. A stable oscillator in a satellite may be used to seek this timing error. In any transmission between satellite and earth, the time Δt_s introduces a variable advance or delay which appears to the observer as a phase-modulated signal. The phase advance in cycles due to the time variation is $f\Delta t_s$ where f is the oscillator frequency. The time derivative of this gives the corresponding frequency shift. Substituting (5), differentiating, and solving for the relative frequency shift results in

$$\frac{\Delta f}{f} = \frac{v}{c^2}[(dS/dt)\cos\gamma - S(d\gamma/dt)\sin\gamma]. \quad (6)$$

The maximum values of dS/dt and $Sd\gamma/dt$ are of the order of the satellite's orbital velocity. Optimum sensitivities are thus obtained with low-altitude satellites and the expression in the brackets then has a maximum value of the order of 10 km/sec. Satellite transmission frequencies have been measured[8] to 1 part in 10^8, and should therefore permit the detection of an ether drift of the order of 100 km/sec. However, the frequency shift in (6) must compete with the Doppler shift and other sources of frequency variation, such as drift. Since the Doppler shift is of the order of the orbital velocity divided by c for most of the path of a low-altitude satellite, the maximum shift in (6) is v/c times smaller. Nevertheless, re-examination of a sufficiently

* Received by the IRE, March 17, 1960.

[1] J. P. Cedarholm and C. H. Townes, "A new experimental test of special relativity," *Nature*, vol. 184, pp. 1350–1351; October 31, 1959.

[2] H. E. Ives, "Derivation of the Lorentz transformations," *Phil. Mag.*, vol. 36, pp. 392–403; June, 1945.

[3] H. E. Ives, "The behavior of an interferometer in a gravitational field, II. Application to a planetary orbit," *J. Opt. Soc. Am.*, vol. 38, pp. 413–416; April, 1948.

[4] H. E. Ives, "The behavior of an interferometer in a gravitational field," *J. Opt. Soc. Am.*, vol. 29, pp. 183–187; May, 1939.

[5] J. C. Maxwell, "Ether," *Enc. Brit.*, 9th ed., vol. 8; 1878.
W. D. Niven, Ed., "The Scientific Papers of James Clerk Maxwell," Dover Publications, Inc., New York, N. Y., vol. 2, p. 763; 1890.
Anonymous, "Clerk Maxwell and the Michelson experiment," *Nature*, vol. 125, p. 566; April, 1930.

[6] K. F. Bottlinger, "Über eine astronomische Prüfungsmöglichkeit des Relativitätsprinzips," *Astronomische Nachrichten*, Band 211, No. 5051, columns 239–240; 1920.

[7] L. Courvoisier, "Ableitung der 'absoluten' Erdbewegung aus beobachteten Längen der Jupiter-Satelliten," *Astronomische Nachrichten*, band 239, nr. 5715, columns 33–38; 1930.

[8] M. Bernstein, G. H. Gougoulis, O. P. Layden, W. T. Scott, and H. D. Tanzman, "Satellite Doppler measurements," PROC. IRE, vol. 46, pp. 782–783; April, 1958.

large body of existing data may permit detection of an ether drift, or the establishment of an upper limit for one.

Use of an atomic clock should improve accuracy by increasing frequency resolution and oscillator stability. The improvement may be sufficient to give significant results with widely separated earth-bound clocks by simultaneous frequency measurements of the same radio transmission. Such comparisons are now being made in this country and in England for other purposes.[9]

A direct measurement of a variation in transmission time, such as the timing error in (5), may be made as suggested elsewhere[10] by precisely keying an oscillator in time. Measurement of the keyed periods by the observer is independent of frequency variations due to Doppler shift, drift, or other causes. With an atomic clock having a stability of 1 part in 10^{10} per day, a total variation in the keyed periods of ± 8.64 μs per day is detectable. A satellite with a period of one day hovers at an altitude of about 36,000 km. For an observer directly underneath, the minimum detectable ether drift in the plane of the satellite's orbit is, from (5), 21.6 km/sec. Sensitivity may be increased by increasing the satellite's distance provided the clock stability can be maintained over the longer orbital period. The ecliptic component timing error may be differentiated from the parameters of the satellite's orbit because the component's phase varies 360° per year. A more direct comparison is obtained by simultaneously measuring the satellite's distance S with an out-and-back radio signal by using the satellite as a beacon.

Regardless of the question of an ether, it is of scientific interest to measure the one-way velocity of light with at least the same precision as the measured average of a two-way signal. The apparent neglect of the one-way measurement, despite the means at hand and the current preparations for related experiments which are more elaborate and advanced, attests to the almost universal, but premature, acceptance of the second postulate of the special theory of relativity.

MARTIN RUDERFER
Dimensions, Inc.
Brooklyn 4, N. Y.

[9] L. V. Essen, J. V. L. Parry, and J. A. Pierce, "Comparison of caesium resonators by transatlantic radio transmission," *Nature*, vol. 180, pp. 526–528; September 14, 1957.
[10] J. T. Anderson, "Determination of the orbit of an artificial satellite," PROC. IRE, vol. 47, pp. 1658–1659; September, 1959.

Microwave Detection and Harmonic Generation by Langmuir-Type Probes in Plasmas*

The demodulation of microwave signals ($f \sim 10{,}000$ mc), when they are impressed upon a Langmuir-type metallic probe in contact with an ionized gaseous medium, has been examined. The plasma was that which forms in the negative glow region of a cold-cathode dc discharge established in helium or neon at pressures ~1–10 mm Hg. The metallic probe was generally a 0.5-cm length of 1.0-mil tungsten wire and was the extension of the center conductor of a coaxial microwave cable (TEM mode). A change in the "continuous" probe current, as the amplitude of the microwave electric potential varied, indicated demodulation.

The nonlinear volt-ampere characteristic of a probe immersed in a plasma is well known and would predict a rectification effect for alternating voltages similar to that observed for the point contact semiconductor diode. This effect has been proposed since at least 1916[1] for the demodulation of low-frequency electrical waves. The present interest stems from recent measurements[2] of the electron temperature in the negative glow plasma established in helium, which indicates quite a low temperature, ~400°K, approaching that of the gas, 300°K. A low effective temperature for the charge carriers (for our case electrons) will lead to a sharp "knee" in the volt-ampere characteristics of the metallic probe. This effect is clearly shown in Fig. 1. Here, the oscilloscopic presentation of probe current, while the probe voltage is swept at a low audio rate, is compared with the current flowing in a conventional 1N23B crystal diode treated in similar fashion. Note that both curves have sharp and similar knees which would predict equivalent sensitivity for demodulation of radio-frequency waves, provided that each curve retained its shape and significance at the higher frequencies.

In one of several arrangements it was possible to impress a pulsed microwave signal (9375 mc with 4-μsec pulse duration) alternately on the metallic probe or on the plasma medium surrounding the probe. Fig. 2 shows the resulting demodulated pulses. The crystal detected pulse is displayed in Fig. 2(c) for purposes of comparison. Fig. 2(a), with microwave energy present only in the plasma, shows a relatively slow response with time constant ~ one microsecond. The essential details of this response may be explained by an alteration of the temperature of the plasma electrons while absorbing microwave energy,[3] and an accompanying change in plasma space potential. When the microwave is impressed on the probe an additional response is noted in Fig. 2(b) at the time of application and removal of the pulse. The rapidity of this response is limited only by the oscilloscope and circuitry.

Of particular interest is the sensitivity of the gaseous discharge detector in comparison with a conventional 1N23B crystal diode. When both types of detectors were tuned for optimum output in equivalent mounts and for incident microwave power

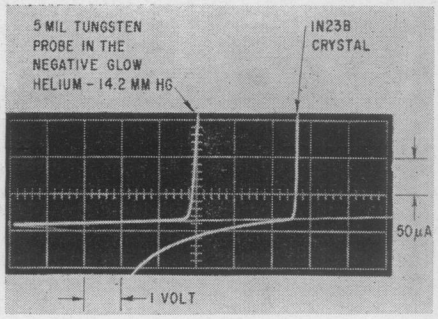

Fig. 1—Comparison of metallic probe and semiconductor diode volt-ampere characteristics with voltage swept at a low audio frequency.

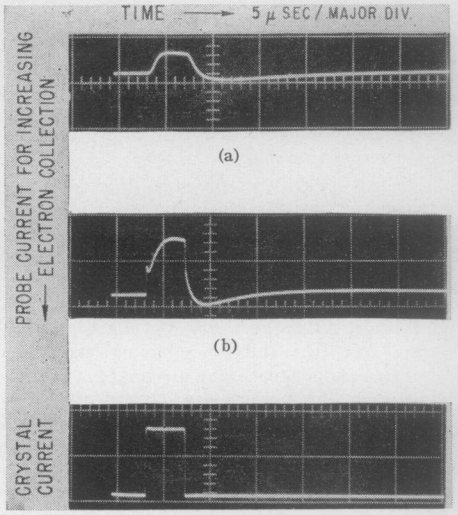

Fig. 2—Video response of Langmuir-type probes immersed in a negative glow plasma established in helium at a pressure of 5 mm Hg.

≈0.1 milliwatt, the crystal detector required approximately 3 db less power for equal response. The minimum detectable signal or noise level of the discharge detector was not examined in these tests. When the cold-cathode discharge plasma was established in neon instead of helium, the discharge detector was approximately 13 db inferior to the crystal.

The magnitude of the fast response, described above, was examined as a function of the incident microwave power. In all cases, the response of the discharge detector for low microwave powers, ≥ 10 mw, followed closely the square law expected from a semiconductor diode.

The above effects suggest a form of rectification between the metallic probe and the plasma wherein the nonlinearity of the device is active for each cycle of alternation of the incident microwave. The generation of waves harmonic in frequency to the incident microwave is immediately suggested. In an appropriately arranged K-band crystal detector mount tuned to 18,750 mc, an almost square pulse of microwave energy having rapid rise and fall was detected, which coincided in time with an incident microwave pulse at 9375 mc to the discharge detector. However, this frequency multiplier was found inferior to a semiconductor diode, 1N23B, by about 16 db in the ability to generate second harmonic energy. A neon-

* Received by the IRE March 30, 1960.

[1] P. C. Hewitt, "Method of, and Apparatus, for, Translating Electrical Variations," U. S. Pat. No. 1,144,596; June 29, 1915.
[2] J. M. Anderson, "Ultimate and secondary electron energies with a negative glow of a cold-cathode discharge in helium," to be published in the *J. Appl. Phys.*; March, 1960.
[3] J. M. Anderson and L. Goldstein, "Interaction of electromagnetic waves of radio-frequency in isothermal plasmas," *Phys. Rev.*, vol. 100, pp. 1037–1046; November, 1960.

filled discharge detector was 17 db inferior to the crystal under similar circumstances. In these second-harmonic measurements, circumstances occasioned a hollow-cathode type of discharge as the only form employed. Later, electrons in this discharge type were found to have a characteristically high temperature, ~1000°K. Most probably, a discharge detector having a plane cathode, as used in the work associated with Figs. 1 and 2, would show a greater efficiency for harmonic generation, but such was not reexamined.

It may be mentioned that a portion of the experimental results reported by M. Uenohara, *et al.*,[4] and by J. R. Baird and P. D. Coleman[5] might possibly be explained on the basis of that given for the above experiments, since metallic electrodes were present in their discharge tubes. However, the above described detector is presumably dissimilar to one of current interest described by Udelson and by Gould,[6] wherein the dc discharge current sustaining the cold-cathode discharge is altered when microwave energy is incident on one or more plasma regions of the discharge.

J. M. Anderson
General Electric Res. Lab.
P. O. Box, 1088
Schenectady, N. Y.

[4] M. Uenohara, M. Uenohara, T. Masutani, and K. Inada, "A new high-power frequency multiplier," Proc. IRE, vol. 45, pp. 1419–1420: October, 1957.
[5] J. R. Baird and P. D. Coleman, "Millimeter waves," Polytechnic Institute of Brooklyn, N. Y., Microwave Res. Inst., *Symposia Series*, vol. 9, pp. 289–300; March, 1959.
[6] B. J. Udelson, "Effect of microwave signals incident upon different regions of a dc hydrogen glow discharge," *J. Appl. Phys.*, vol. 28, pp. 380–381; March, 1959. L. Gould, U. S. Army Signal Corps, Engrg. Labs., Fort Monmouth, N. J., Signal Corps Task No. 323B, Tech. Memo No. M-1836; October 31, 1956.

A New Use of the Junction Transistor as a Pulse-Width Modulator*

Price's paper[1] reports that transistors can be used as a pulse-width modulator in a saturation region, utilizing the minority carrier storage effect. That technique is described with a "selected point-contact transistor" whose current gain, alpha, is larger than five. The collector potential is modulated, using a common base configuration.

This paper describes a new method of pulse-width modulation which modulates the base pulse current in a common emitter configuration. This new method is more suited to junction transistors. It is expected, therefore, that a more applicable and practical method of modulation with good linearity and effectiveness will be obtained.

If enough input pulse current is supplied to saturate the transistor, each output pulse maintains a constant amplitude during the storage time, due to the fact that the collector load resistance and collector bias supply voltage are fixed.

When the input current is modulated by audio frequencies at the base of the transistor in saturation region, only the width of output pulses varies in accordance with the input modulation signal. Thus the pulse amplitude modulation at the input is transformed to the pulse-width (or phase) modulation at the output automatically.

A simplified circuit for this method is shown in Fig. 1. The modulated input and output voltage waveforms are shown in Fig. 2, where the pulse-width is 10 microseconds, repetition frequency is 10 kilocycles, R_C is 4.7 kilohms and E_C is 6 volts. In Fig. 3, the demodulated sine wave with a frequency of 100 cycles is illustrated. The distortion factor of the wave is about 5.5 per cent. Using a proper circuit, it was found that, according to the oscillographic observation, the distortion factor of the sine waves up to 10 kilocycles is almost the same as that of the wave at 100 cycles.

Triggering a flip-flop by the differentiated impulse of the output modulated pulse, as shown in Fig. 4, the distortion factor of the system will become less than 5 per cent.

This method also serves as a simple pulse-delaying circuit adaptable to various pulse and logic circuits.

Plans are being made for estimating the signal-to-noise ratio and limit of modulation factor at any given circuit and frequency conditions.

The author is grateful to Dr. H. Kuroda and Dr. T. Nakano for their valuable discussions.

I. Tagoshima
Tech. Res. Lab.
Japan Broadcasting Corp.
Kinuta, Setegaya, Tokyo, Japan

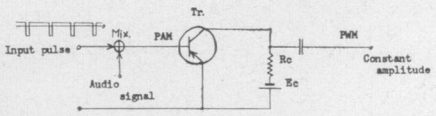

Fig. 1—Simplified PWM circuit.

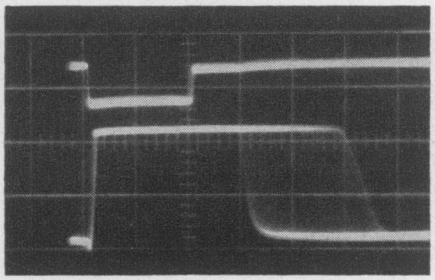

Fig. 2—Modulated pulse waves. Input voltage, PAM (upper) and output voltage, PWM (lower) of this method, using a low frequency junction transistor. Input alloy width is 00 μsec.

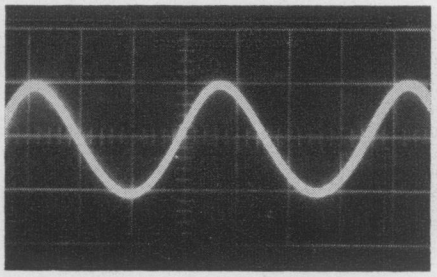

Fig. 3—Demodulated sine wave (100 cycles).

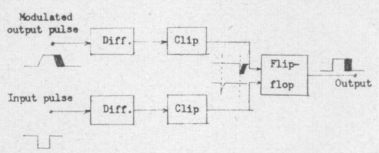

Fig. 4—Block diagram of a pulse readjusting circuit.

* Received by the IRE, March 28, 1960.
[1] J. C. Price, "A conductivity storage transistor pulse width modulator," *Elec. Engrg.*, vol. 30, pp. 88–90; February, 1958.

On the Uniqueness Theorem for Electromagnetic Fields*

The following proof of the uniqueness theorem of the solution of boundary value problems in electromagnetic field theory will be based on the general ideas of uniqueness theorem proof given by Stratton.[1] However, this proof will be original in a way, as it will consider also the case of resonant modes and mixed boundary conditions in the steady-state case, which were not considered by Stratton.

Let V be a region of space bounded by a closed surface S. It will be assumed that V is an isotropic medium with the scalar paramaters μ, ϵ, σ as arbitrary functions of position. Let $(\overline{E}_1; \overline{H}_1)$ and $(\overline{E}_2; \overline{H}_2)$ be two solutions of the field equations with harmonic time variation $e^{-i\omega t}$. Assuming linearity of the field equations, the difference field $\overline{E}=\overline{E}_1-\overline{E}_2$ and $\overline{H}=\overline{H}_1-\overline{H}_2$ is also a solution of the boundary value problem. Let us assume that the sources lie entirely outside the region V.

From Maxwell's equations with harmonic time variation one can get the following relation for the complex Poynting vector:[1]

$$\nabla\cdot(\overline{E}\times\overline{H}^*) = -\sigma\overline{E}\cdot\overline{E}^* + i2\omega\left(\frac{\mu}{2}\overline{H}\cdot\overline{H}^* - \frac{\epsilon}{2}\overline{E}\cdot\overline{E}^*\right). \quad (1)$$

Taking the volume integral on both sides of (1), and separating into real and imaginary pairs we get:

$$\mathrm{Re}\oiint_S(\overline{E}\times\overline{H}^*)\cdot\bar{n}\,dS = -\int_V \sigma E^2 dV \quad (2a)$$

$$\mathrm{Im}\oiint_S(\overline{E}\times\overline{H}^*)\cdot\bar{n}\,dS = 2\omega\int_V\left(\frac{\mu}{2}H^2 - \frac{\epsilon}{2}E^2\right)dV. \quad (2b)$$

If we prescribe $\bar{n}\times\overline{E}_1=\bar{n}\times\overline{E}_2$ *or* $\bar{n}\times\overline{H}_1=\bar{n}\times\overline{H}_2$ on the surface S, the left-hand side integrals in (2) will vanish since

$$(\overline{E}\times\overline{H}^*)\cdot\bar{n} = (\bar{n}\times\overline{E})\cdot\overline{H}^* = -(\bar{n}\times\overline{H}^*)\cdot\overline{E}, \quad (3)$$

* Received by the IRE, March 7, 1960.
[1] J. A. Stratton, "Electromagnetic Theory," McGraw-Hill Book Co., Inc., New York, N. Y., pp. 137, 486–488; 1941.

and $\overline{E}=\overline{E}_1-\overline{E}_2$, and $\overline{H}=\overline{H}_1-\overline{H}_2$. The integrals on the left-hand side of (2) will also vanish in the mixed boundary conditions case in which $\bar{n}\times\overline{E}_1=\bar{n}\times\overline{E}_2$ is prescribed over *part* of the closed surface S and $\bar{n}\times\overline{H}_1=\bar{n}\times\overline{H}_2$ is prescribed over the *rest* of the surface S. Therefore (2) will become

$$\int_V \sigma E^2 dV = 0, \tag{4a}$$

$$\int_V \frac{\mu}{2} H^2 dV = \int_V \frac{\epsilon}{2} E^2 dV. \tag{4b}$$

We must distinguish between two different cases in (4). a) $\sigma\neq 0$. The medium has losses. In this case we see from (4a) that since $\sigma>0$, we will have to have throughout the volume V, $\overline{E}=\overline{E}_1-\overline{E}_2=0$. Using this in (4b) we also get $\overline{H}=\overline{H}_1-\overline{H}_2=0$ throughout the volume V. Therefore, in those cases the two solutions will be identical. b) $\sigma=0$. The medium does not have any losses. In this case (4a) becomes an identity and only (4b) is left. From this equation we see that the differences $\overline{E}_1=\overline{E}_1-\overline{E}_2$ and $\overline{H}=\overline{H}_1-\overline{H}_2$ do not have to be identically zero throughout the volume V. The only requirement in (4b) by itself is that the total average electric energy of the difference field will be equal to the total average magnetic energy of the difference field; in other words it is required that the difference electromagnetic field between the two solutions will be a resonant mode. Only in cases where we do not have any resonant modes will we get a unique solution. One such case is the case of an unbounded region with radiation conditions prescribed at infinity.[2]

Let us summarize the uniqueness theorem:

> A harmonic time-varying electromagnetic field is uniquely determined within a *lossy* bounded region V, by prescribing *one* of the following on the surrounding surface S:
>
> 1) the tangential component of the electric vector.
> 2) the tangential component of the magnetic vector,
> 3) the tangential component of the electric vector over part of the surface S, and the tangential component of the magnetic vector over the rest of the surface S.

In case of a *lossless* bounded region V, the electromagnetic field will *not* be uniquely determined by the above, since by adding any number of resonant modes to a solution, a new solution will be found.

In case of an *unbounded* region V, with radiation conditions at infinity, any one of the above will determine a unique solution.

H. Unz
Elect. Engrg. Dept.
University of Kansas
Lawrence, Kans.

[2] W. K. Saunders, *Proc. Natl. Acad. Sciences*, vol. 38, pp. 342–348; April, 1952.

J-Band Strip-Line *Y* Circulator*

A strip-line Y circulator has been realized with successful results in the L-band case.[1,2]

The lower the operating frequency of the circulator is, the more difficult the realization of the circulator becomes, because of the lowering of the figure of merit which comes from the characteristics of both polycrystalline YIG and the strip-line. The triplate strip-line Y circulators in the lower bands of the UHF region have been tested in order to find out their practical lowest operating frequency, and good results have been obtained even in the J-band (from 350 mc to 530 mc), which is reported later in this letter. It has also been ascertained that the practical lowest limit of the operating frequency of the circulator is expected to be at some frequency band in the VHF region.

According to the experimental results of the circulator made up for the several bands in the UHF region, the figures of merit (the backward transmission loss in decibels upon the forward transmission loss in decibels), the necessary applied magnetic fields by Alnico magnets, and the sizes of the devices (in which three type n connectors, three coaxial line-strip line junctions, three Alnico magnets, and two adjustable pole pieces are included), are given in Fig. 1 against the operating free-space wavelength respectively. In the case of the circulator made up to 360-mc use in the J-band they are about 100, about 1250 oersteds, $6\frac{3}{4}$ inches in diameter (2 inches in height), respectively.

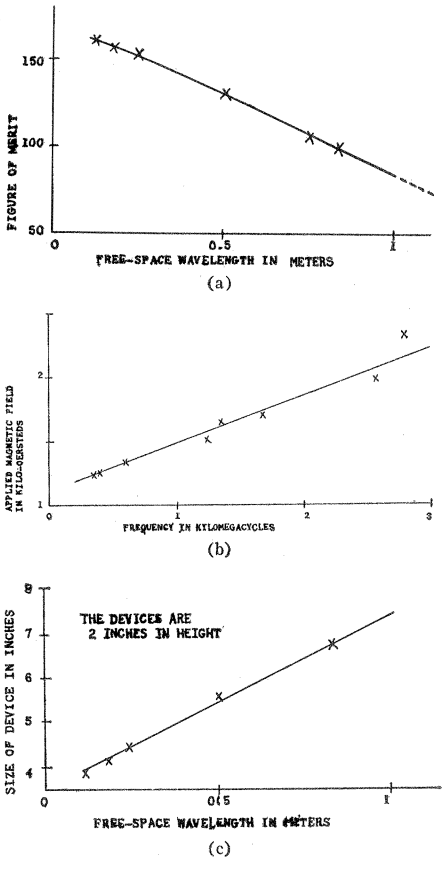

Fig. 1.

When a wave of frequency 360 mc enters, for example, through arm 1 from a matched generator, it comes out from arms 2 and 3 terminated by matched detectors. Transmission losses are shown against the applied dc magnetic field in Fig. 2. When the external dc magnetic field corresponding to point A (about 1250 oersteds) in this figure is applied, the clockwise circulator is completed in this case. In practice, three Alnico magnets, having a magnetic field corresponding to the point A, are set to the strip-line Y junction. The frequency characteristics of the circulator are shown in Fig. 3.

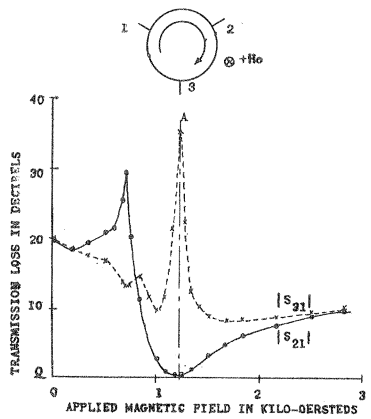

Fig. 2.

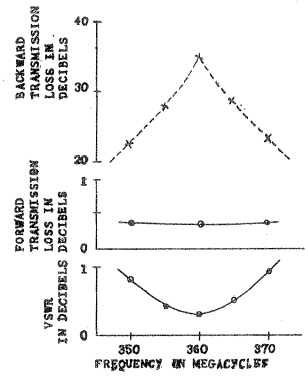

Fig. 3.

These data are obtained for the circulator with type n coaxial connectors. Typical performance is within 0.4-db insertion loss over 20-db isolation with VSWR less than 1 db over 7 per cent bandwidth of the center frequency in J-band, and is 0.3_5 to 34.8 db with VSWR 0.3 db at the center of the band. We can expect to get better characteristics when the strip-line circulator is used without the coaxial connectors and the coaxial strip-line junctions. The same type of circulator can be made in the case of the other types of strip-line. Also, a microwave switch can be easily made by the modulation of the external magnetic field.

S. Yoshida
Matsuda Res. Lab.
Tokyo Shibaura Electric Co., Ltd.
Kawasaki, Kanagawa, Japan

* Received by the IRE, March 29, 1960.

[1] L. Davis, Jr., U. Milano, and J. Saunders, "A strip-line L-band compact circulator," Proc. IRE, vol. 48, pp. 115–116; January, 1960.

[2] S. Yoshida, "Strip-line Y circulator," Proc. IRE, vol. 48, pp. 1337–1338; July, 1960.

Interaction of Two Microwave Signals in a Ferroelectric Material*

A conventional degenerate mode parametric amplifier was used as a research tool to study the ferroelectric interaction with two microwave signals. Certain interesting results were obtained, namely, that there was an exchange of energy from the pump frequency to the signal frequency in the ferroelectric material via an idler frequency. Results are shown in Table I.

There was too much loss in the system at 1200 mc and 820 mc to obtain any gain; in fact, the insertion loss of the microwave circuit with material used was 7.5 db. Removing the pump frequency removes the idler and also lowers the amplitude of the signal frequency. The operation is very similar to a parametric amplifier with a low-cutoff frequency or lossy varactor.

TABLE I

f_s	f_p	Relative Amplitude of the Idler to the Signal Frequency	Pump Power
2600 mc	5200 mc	−31 db	1 watt
1200 mc	2400 mc	−6 db	120 mw
820 mc	1640 mc	−6 db	150 mw

The ferroelectric material was Barium Titanate of the polycrystalline type, Aerovox Body 90, operating at room temperature below its Curie point. A small chip, 0.005 inch thickness and 0.010 inch on a side, was used in a modified microwave crystal holder. The capacity of the sample was 2.2 $\mu\mu$f.

It does appear that the permittivity of the material can be varied at a microwave frequency rate; hence, the material becomes a variable capacity, thus making possible the basic element for a ferroelectric parametric amplifier.

The author wishes to acknowledge the stimulating discussions with Dr. H. Diamond and T. H. Butler of the University of Michigan.

IRVING GOLDSTEIN, MANAGER
Solid-State Physics Branch
Raytheon Missile Systems Div.
Bedford, Mass.

* Received by the IRE, April 11, 1960.

Contributors

Bruce B. Barrow (S'52–M'56–SM'59) was born on April 12, 1929, in Danville, Pa. He attended the Carnegie Institute of Technology, Pittsburgh, Pa., on a George Westinghouse Scholarship, and received the B.S.E.E. and M.S.E.E. degrees in 1950. He was awarded a Tau Beta Pi Fellowship for graduate study at the Massachusetts Institute of Technology, Cambridge, where he also taught in the Department of Electrical Engineering and worked on the staff of the Servomechanisms Laboratory. During this time, he was awarded a Fulbright Scholarship for a year of study at the Delft Institute of Technology in The Netherlands. In his last years at M.I.T. he worked in the Nuclear Instrumentation Group under the direction of Prof. T. S. Gray, and in 1955 he received the E.E. degree. His thesis was concerned with nuclear reactor instrumentation, and he has consulted for the General Electric Company in this field.

B. B. BARROW

In 1955, he joined Hermes Electronics Co., Cambridge, Mass., where he worked mainly on problems concerned with various communications systems, including the ACE High network now being constructed in Europe for SHAPE. Since 1958, he has been on leave with the SHAPE Air Defense Technical Center, The Hague, where he is studying improved methods of transmitting digital data over fading radio paths.

Mr. Barrow is a member of the Nederlands Radiogenootschap, Sigma Xi, and Tau Beta Pi.

Robert L. Carbrey (M'45) was born in Denver, Colo., on April 23, 1917. He received the B.S.E.E. degree with honors from the University of Colorado, Boulder, in 1940.

R. L. CARBREY

He joined the Bell Telephone Laboratories' outside plant department in 1940, where he engaged in work on coaxial and toll telephone cables. During World War II, he transferred to the radio research department where he worked on radar and pulse position modulation receivers, as well as single-sideband receivers. Since his transfer to the transmission research department at Murray Hill, N. J., in 1944, he has been engaged in work on a variety of pulse code modulation terminals and repeaters, except for an interval, during which time he worked on the design of time separation multiplexed speech interpolation systems.

Mr. Carbrey is a member of Tau Beta Pi and Eta Kappa Nu.

❖

Martin L. Cohen (M'60) was born in New York, N. Y., on May 20, 1929. He received the B.E.E. degree from Cornell University, Ithaca, N. Y., in 1952.

From 1952 to 1956, he worked for Raytheon Manufacturing Company, Newton, Mass., on the development of nonmicrophonic vacuum tubes and test equipment for microwave tubes. Before joining Arthur D. Little, Inc., Cambridge, Mass., in 1957 as a member of the Advanced Research Division, he studied applied mathematics and switching theory at Harvard University, Cambridge. His work at Arthur D. Little has been in the experimental development of superconductive computer elements, which has included research with the wire-wound cryotron and on the properties of vacuum-deposited superconductive films.

M. L. COHEN

❖

Sid Deutsch (A'46–M'55) was born in New York, N. Y., on September 19, 1918. He received the B.E.E. degree in 1941 from Cooper Union, New York, N. Y., and the M.E.E. and D.E.E. degrees in 1947 and 1955 from the Polytechnic Institute of Brooklyn, Brooklyn, N. Y.

S. DEUTSCH

From 1935 to 1944, he was an electric motor technician and designer of electromechanical equipment and then served with the U. S. Navy until 1946. He was an electronics engineer from 1950 to 1954 at the Polytechnic Research and Development Company, Brooklyn, N. Y., and then joined